Supplemental Information for "Experimental Test of the Greenberger–Horne–Zeilinger-type Paradoxes in and beyond Graph States"

CONTENTS

1. ADDITIONAL THEORETICAL INFORMATION

A. The detail proof for Theorem 1

For a m-vertices graph, without loss generality, we focus on the vertex labeled by 1. For the vertex 1, it connects with other $n-1$ vertices ($3 \leq n \leq m$), which are labeled by $2, 3, \cdots, n$, respectively. We then define C_i^j as the *connectivity* of the vertices i and j, $C_i^j = C_j^i = 1$ means the vertices i and j are connected, and $C_i^j = C_j^i = 0$ means they are disconnected. Let's define the following Hamiltonian

$$\mathcal{H} = -\sum_{i=1}^{n} S_i, \tag{1}$$

where

$$S_i = \sigma_x^i \prod_{j\neq i} (\sigma_z^j)^{C_i^j}, \quad (i, j = 1, 2, \cdots, m) \tag{2}$$

is the stabilizing operator for the vertex i, $\vec{\sigma} = (\sigma_x, \sigma_x, \sigma_z)$ is the Pauli matrix vector, and

$$(\sigma_z^j)^{C_i^j} = \begin{cases} \sigma_z^j, & \text{if } C_i^j = 1, \\ \mathbb{1}, & \text{if } C_i^j = 0, \end{cases} \tag{3}$$

For convenient, we have listed the explicit forms of operators S_i's in detail in the Table 1. The ground state of $\mathcal{H}$ is denoted by $|G\rangle$, for which we have

$$S_i|G\rangle = +|G\rangle, \quad i \in \{1, 2, \cdots, n\}. \tag{4}$$

and

$$\mathcal{H}|G\rangle = -n\,|G\rangle. \tag{5}$$

For the quantum state $|G\rangle$, we have the following theorem.

Supplementary Table 1. The explicit forms of stabilizing operators for vertex 1 to vertex n. For example, $S_1 = \sigma_x^1 \sigma_z^2 \sigma_z^3 \cdots \sigma_z^n$.

	1	2	3	4	$\cdots$	$n-2$	$n-1$	n
S_1	σ_x	σ_z	σ_z	σ_z	$\cdots$	σ_z	σ_z	σ_z
S_2	σ_z	σ_x	$\sigma_z^{C_2^3}$	$\sigma_z^{C_2^4}$	$\cdots$	$\sigma_z^{C_2^{n-2}}$	$\sigma_z^{C_2^{n-1}}$	$\sigma_z^{C_2^n}$
S_3	σ_z	$\sigma_z^{C_3^2}$	σ_x	$\sigma_z^{C_3^4}$	$\cdots$	$\sigma_z^{C_3^{n-2}}$	$\sigma_z^{C_3^{n-1}}$	$\sigma_z^{C_3^n}$
S_4	σ_z	$\sigma_z^{LC_4^2}$	$\sigma_z^{LC_4^3}$	σ_x	$\cdots$	$\sigma_z^{LC_4^{n-2}}$	$\sigma_z^{LC_4^{n-1}}$	$\sigma_z^{LC_4^n}$
$\vdots$	$\vdots$	$\vdots$	$\vdots$	$\vdots$	$\vdots$	$\vdots$	$\vdots$	$\vdots$
S_{n-2}	σ_z	$\sigma_z^{C_{n-2}^2}$	$\sigma_z^{C_{n-2}^3}$	$\sigma_z^{C_{n-2}^4}$	$\cdots$	σ_x	$\sigma_z^{C_{n-2}^{n-1}}$	$\sigma_z^{C_{n-2}^n}$
S_{n-1}	σ_z	$\sigma_z^{C_{n-1}^2}$	$\sigma_z^{C_{n-1}^3}$	$\sigma_z^{C_{n-1}^4}$	$\cdots$	$\sigma_z^{C_{n-1}^{n-2}}$	σ_x	$\sigma_z^{C_{n-1}^n}$
S_n	σ_z	$\sigma_z^{C_n^2}$	$\sigma_z^{C_n^3}$	$\sigma_z^{C_n^4}$	$\cdots$	$\sigma_z^{C_n^{n-2}}$	$\sigma_z^{C_n^{n-1}}$	σ_x

Theorem 1.—(i) For n is *odd*, the GHZ-type paradox or the sharp contradiction "$+1_{\rm C} = -1_{\rm Q}$" can be arisen from the following $n+1$ operators:

$$\{S_1, \quad (-1)^{a_i} S_1^{a_i} S_i S_{i+1}, \quad S_1^{a_n} S_j\}, \quad i = 2, \ldots, n-1, \quad j = 2, n, \tag{6}$$

where

$$a_l = 1 + \sum_{k \neq l} C_k^{k+1}, \quad (k = 2, \cdots, n-1, \quad l = 2, \cdots, n) \tag{7}$$

and

$$S_1^{a_i} = \begin{cases} S_1, & \text{if } \mathrm{Mod}[a_i, 2] = 1, \\ \mathbb{1}, & \text{if } \mathrm{Mod}[a_i, 2] = 0. \end{cases} \tag{8}$$

(ii) For n is *even*, the GHZ-type paradox or the sharp contradiction "$+1_{\rm C} = -1_{\rm Q}$" can be arisen from the following n operators:

$$\{S_1, \quad (-1)^{a_i} S_1^{a_i} S_i S_{i+1}\}, \quad i = 2, \ldots, n, \tag{9}$$

where

$$a_l = 1 + \sum_{k \neq l} C_k^{k+1}, \quad (k, l = 2, \cdots, n) \tag{10}$$

and

$$S_{n+1} = S_2, \quad C_n^{n+1} = C_n^2. \tag{11}$$

Proof. (i) n is *odd*.

Step 1.—Let us prove that quantum prediction is "-1". For simplicity, let us denote F_k as the k-th operator in the set of $n+1$ operators $\{S_1,\ (-1)^{a_i} S_1^{a_i} S_i S_{i+1},\ S_1^{a_n} S_j\}$, i.e.,

$$F_k = [\{S_1,\ (-1)^{a_i} S_1^{a_i} S_i S_{i+1},\ S_1^{a_n} S_j\}]_k. \tag{12}$$

Based on Eq. (4), it is easy to have

$$[F_1 = S_1]|G\rangle = +1|G\rangle, \tag{13a}$$
$$[F_i = (-1)^{a_i} S_1^{a_i} S_i S_{i+1}]|G\rangle = (-1)^{a_i}|G\rangle, \quad (i = 2, \ldots, n-1) \tag{13b}$$
$$[F_n = S_1^{a_n} S_2]|G\rangle = +1|G\rangle, \tag{13c}$$
$$[F_{n+1} = S_1^{a_n} S_n]|G\rangle = +1|G\rangle, \tag{13d}$$

Then we obtain the quantum prediction as

$$\mathcal{Q} = \prod_{k=1}^{n+1} \langle G|F_k|G\rangle = (-1)^{\sum_{i=2}^{n-1} a_i}. \tag{14}$$

To acquire the total of the parameter a_i's, we use the definition of the connectivity in (10), and recombine the summations of C_k^{k+1}:

$$\begin{aligned}\sum_{i=2}^{n-1} a_i &= a_2 + a_3 + a_4 + \cdots + a_{n-1} \\ &= (1 + \sum_{k\neq 2} C_k^{k+1}) + (1 + \sum_{k\neq 3} C_k^{k+1}) + (1 + \sum_{k\neq 4} C_k^{k+1}) + \cdots + (1 + \sum_{k\neq n-1} C_k^{k+1}) \\ &= (n-2) + (n-3)(C_2^3 + C_3^4 + C_4^5 + \cdots + C_{n-2}^{n-1} + C_{n-1}^n),\end{aligned} \tag{15}$$

However, because n is odd, $(n-2)$ must also be odd and $(n-3)$ be even. Consequently, $\sum_{i=2}^{n-1} a_i$ is an odd number, and the quantum prediction is

$$\mathcal{Q} = (-1)^{\sum_{i=2}^{n-1} a_i} = -1. \tag{16}$$

Step 2.—Let us prove that classical prediction is "+1". In Table 2, we have listed the explicit forms for the operators F_k. For examples, for $k=1$ we have

$$F_1 = S_1 = \sigma_x^1 \otimes \sigma_z^2 \otimes \sigma_z^3 \otimes \cdots \otimes \sigma_z^{n-1} \otimes \sigma_z^n. \tag{17}$$

For $k=2$, we have

$$F_2 = (-1)^{a_2} S_1^{a_2} S_2 S_3 = (-1)^{a_2}\ [(\sigma_x^1)^{a_2} \otimes (\sigma_z^2)^{a_2} \sigma_x^2 (\sigma_z^2)^{C_3^2} \otimes (\sigma_z^3)^{a_2} (\sigma_z^3)^{C_2^3} \sigma_x^3 \otimes \prod_{j=4}^{n} \sigma_z^{a_2 + C_2^j + C_3^j}], \tag{18}$$

due to

$$(\sigma_z)^\ell \sigma_x = -(\sigma_z)^{\ell-1} \sigma_x \sigma_z = (-1)^\ell\ \sigma_x (\sigma_z)^\ell, \tag{19}$$

with ℓ being an integer number, we then obtain

$$(-1)^{a_2} (\sigma_z^2)^{a_2} \sigma_x^2 = \sigma_x^2 (\sigma_z^2)^{a_2}. \tag{20}$$

Substituting Eq. (20) into Eq. (18), we then have

$$\begin{aligned}F_2 &= (\sigma_x^1)^{a_2} \otimes \sigma_x^2 (\sigma_z^2)^{a_2 + C_3^2} \otimes (\sigma_z^3)^{a_2 + C_2^3} \sigma_x^3 \otimes \prod_{j=4}^{n} \sigma_z^{a_2 + C_2^j + C_3^j} \\ &= (\sigma_x^1)^{a_2} \otimes (\sigma_z^2)^{a_2 + C_3^2} \sigma_x^2 \otimes \sigma_x^3 (\sigma_z^3)^{a_2 + C_2^3} \otimes \prod_{j=4}^{n} \sigma_z^{a_2 + C_2^j + C_3^j}.\end{aligned} \tag{21}$$

Based on Eq. (10), it is easy to have

$$a_i + C_i^{i+1} = a_i + C_{i+1}^i = a_n, \quad (i = 2, 3, \cdots, n-1), \tag{22}$$

then Eq. (21) becomes

$$F_2 = (\sigma_x^1)^{a_2} \otimes (\sigma_z^2)^{a_n} \sigma_x^2 \otimes \sigma_x^3 (\sigma_z^3)^{a_n} \otimes \prod_{j=4}^{n} \sigma_z^{a_2 + C_2^j + C_3^j}. \tag{23}$$

which is just the one listed in Table 2. Similarly, one can directly calculate other F_k's, their explicit forms are given in Table 2.

Remark 1.—For the operator F_2, there are two quadratic terms that contain two different Pauli matrices, namely, $(\sigma_z)^{a_n} \sigma_x$ and $\sigma_x (\sigma_z)^{a_n}$. Case (i). If $\mathrm{Mod}[a_n, 2] = 0$, then one has

$$(\sigma_z)^{a_n} \sigma_x = \sigma_x (\sigma_z)^{a_n} = \sigma_x, \tag{24}$$

Supplementary Table 2. The explicit forms of operators F_k, $(k = 1, 2, \cdots, n+1)$. Here n is *odd*.

	1	2	3	4	$\cdots$	$n-2$	$n-1$	n
F_1	σ_x	σ_z	σ_z	σ_z	$\cdots$	σ_z	σ_z	σ_z
F_2	$\sigma_x^{a_2}$	$\sigma_z^{a_n}\sigma_x$	$\sigma_x\sigma_z^{a_n}$	$\sigma_z^{a_2+C_2^4+C_3^4}$	$\cdots$	$\sigma_z^{a_2+C_2^{n-2}+C_3^{n-2}}$	$\sigma_z^{a_2+C_2^{n-1}+C_3^{n-1}}$	$\sigma_z^{a_2+C_2^n+C_3^n}$
F_3	$\sigma_x^{a_3}$	$\sigma_z^{a_3+C_3^2+LC_4^2}$	$\sigma_x\sigma_z^{a_n}$	$\sigma_z^{a_n}\sigma_x$	$\cdots$	$\sigma_z^{a_3+C_3^{n-2}+LC_4^{n-2}}$	$\sigma_z^{a_3+C_3^{n-1}+LC_4^{n-1}}$	$\sigma_z^{a_3+C_3^n+LC_4^n}$
F_4	$\sigma_x^{a_4}$	$\sigma_z^{a_4+LC_4^2+C_5^2}$	$\sigma_z^{a_4+LC_4^3+C_5^3}$	$\sigma_z^{a_n}\sigma_x$	$\cdots$	$\sigma_z^{a_4+LC_4^{n-2}+C_5^{n-2}}$	$\sigma_z^{a_4+LC_4^{n-1}+C_5^{n-1}}$	$\sigma_z^{a_4+LC_4^n+C_5^n}$
$\vdots$	$\vdots$	$\vdots$	$\vdots$	$\vdots$	$\vdots$	$\vdots$	$\vdots$	$\vdots$
F_{n-2}	$\sigma_x^{a_{n-2}}$	$\sigma_z^{a_{n-2}+C_{n-2}^2+C_{n-1}^2}$	$\sigma_z^{a_{n-2}+C_{n-2}^3+C_{n-1}^3}$	$\sigma_z^{a_{n-2}+C_{n-2}^4+C_{n-1}^4}$	$\cdots$	$\sigma_x\sigma_z^{a_n}$	$\sigma_z^{a_n}\sigma_x$	$\sigma_z^{a_{n-2}+C_{n-2}^n+C_{n-1}^n}$
F_{n-1}	$\sigma_x^{a_{n-1}}$	$\sigma_z^{a_{n-1}+C_{n-1}^2+C_n^2}$	$\sigma_z^{a_{n-1}+C_{n-1}^3+C_n^3}$	$\sigma_z^{a_{n-1}+C_{n-1}^4+C_n^4}$	$\cdots$	$\sigma_z^{a_{n-1}+C_{n-1}^{n-2}}$	$\sigma_z^{a_n}\sigma_x$	$\sigma_x\sigma_z^{a_n}$
F_n	$\sigma_x^{a_n}\sigma_z$	$\sigma_z^{a_n}\sigma_x$	$\sigma_z^{a_n+C_2^3}$	$\sigma_z^{a_n+C_2^4}$	$\cdots$	$\sigma_z^{a_n+C_2^{n-2}}$	$\sigma_z^{a_n+C_2^{n-1}}$	$\sigma_z^{a_n+C_2^n}$
F_{n+1}	$\sigma_x^{a_n}\sigma_z$	$\sigma_z^{a_n+C_n^2}$	$\sigma_z^{a_n+C_n^3}$	$\sigma_z^{a_n+C_n^4}$	$\cdots$	$\sigma_z^{a_n+C_n^{n-2}}$	$\sigma_z^{a_n+C_n^{n-1}}$	$\sigma_z^{a_n}\sigma_x$

then Eq. (23) becomes

$$F_2 = (\sigma_x^1)^{a_2} \otimes \sigma_x^2 \otimes \sigma_x^3 \otimes \prod_{j=4}^{n} \sigma_z^{a_2+C_2^j+C_3^j}. \tag{25}$$

Case (ii). If $\mathrm{Mod}[a_n, 2] = 1$, then by using the basic relation of Pauli matrices

$$\sigma_x\sigma_y = i\,\sigma_z, \quad \sigma_y\sigma_z = i\,\sigma_x, \quad \sigma_z\sigma_x = i\,\sigma_y, \quad (i = \sqrt{-1}), \tag{26}$$

one has

$$(\sigma_z)^{a_n}\sigma_x = i\,\sigma_y, \quad \sigma_x(\sigma_z)^{a_n} = -i\,\sigma_y, \tag{27}$$

then Eq. (23) becomes

$$F_2 = (\sigma_x^1)^{a_2} \otimes \sigma_y^2 \otimes \sigma_y^3 \otimes \prod_{j=4}^{n} \sigma_z^{a_2+C_2^j+C_3^j}. \tag{28}$$

Therefore, based on Eqs. (25) and (28), we finally have F_2 as

$$F_2 = (\sigma_x^1)^{a_2} \otimes \Sigma_{x,y}^2 \otimes \Sigma_{x,y}^3 \otimes \prod_{j=4}^{n} \sigma_z^{a_2+C_2^j+C_3^j}, \tag{29}$$

with

$$\Sigma_{x,y} = \begin{cases} \sigma_x, & \text{if } \mathrm{Mod}[a_n, 2] = 0, \\ \sigma_y, & \text{if } \mathrm{Mod}[a_n, 2] = 1. \end{cases} \tag{30}$$

Similarly, one can make the same analysis for other F_k's, with $k = 3, 4, \cdots, n-1$.

Remark 2.—For $k = n$, we have

$$F_n = (\sigma_x^1)^{a_n}\sigma_z^1 \otimes (\sigma_z^2)^{a_n}\sigma_x^2 \otimes \prod_{j=3}^{n} (\sigma_z^j)^{a_n+C_2^j}. \tag{31}$$

Case (i). If $\mathrm{Mod}[a_n, 2] = 0$, then one has

$$(\sigma_x)^{a_n}\sigma_z = \sigma_z, \quad (\sigma_z)^{a_n}\sigma_x = \sigma_x, \tag{32}$$

Supplementary Table 3. Another explicit forms of operators F_k, $(k=1,2,\cdots,n+1)$. Here n is *odd*.

	1	2	3	4	$\cdots$	$n-2$	$n-1$	n
F_1	σ_x	σ_z	σ_z	σ_z	$\cdots$	σ_z	σ_z	σ_z
F_2	$\sigma_x^{a_2}$	$\Sigma_{x,y}$	$\Sigma_{x,y}$	$\sigma_z^{a_2+C_2^4+C_3^4}$	$\cdots$	$\sigma_z^{a_2+C_2^{n-2}+C_3^{n-2}}$	$\sigma_z^{a_2+C_2^{n-1}+C_3^{n-1}}$	$\sigma_z^{a_2+C_2^n+C_3^n}$
F_3	$\sigma_x^{a_3}$	$\sigma_z^{a_3+C_3^2+LC_4^2}$	$\Sigma_{x,y}$	$\Sigma_{x,y}$	$\cdots$	$\sigma_z^{a_3+C_3^{n-2}+LC_4^{n-2}}$	$\sigma_z^{a_3+C_3^{n-1}+LC_4^{n-1}}$	$\sigma_z^{a_3+C_3^n+LC_4^n}$
F_4	$\sigma_x^{a_4}$	$\sigma_z^{a_4+LC_4^2+C_5^2}$	$\sigma_z^{a_4+LC_4^3+C_5^3}$	$\Sigma_{x,y}$	$\cdots$	$\sigma_z^{a_4+LC_4^{n-2}+C_5^{n-2}}$	$\sigma_z^{a_4+LC_4^{n-1}+C_5^{n-1}}$	$\sigma_z^{a_4+LC_4^n+C_5^n}$
$\vdots$	$\vdots$	$\vdots$	$\vdots$	$\vdots$	$\vdots$	$\vdots$	$\vdots$	$\vdots$
F_{n-2}	$\sigma_x^{a_{n-2}}$	$\sigma_z^{a_{n-2}+C_{n-2}^2+C_{n-1}^2}$	$\sigma_z^{a_{n-2}+C_{n-2}^3+C_{n-1}^3}$	$\sigma_z^{a_{n-2}+C_{n-2}^4+C_{n-1}^4}$	$\cdots$	$\Sigma_{x,y}$	$\Sigma_{x,y}$	$\sigma_z^{a_{n-2}+C_{n-2}^n+C_{n-1}^n}$
F_{n-1}	$\sigma_x^{a_{n-1}}$	$\sigma_z^{a_{n-1}+C_{n-1}^2+C_n^2}$	$\sigma_z^{a_{n-1}+C_{n-1}^3+C_n^3}$	$\sigma_z^{a_{n-1}+C_{n-1}^4+C_n^4}$	$\cdots$	$\sigma_z^{a_{n-1}+C_{n-1}^{n-2}}$	$\Sigma_{x,y}$	$\Sigma_{x,y}$
F_n	$\Sigma_{z,y}$	$\Sigma_{x,y}$	$\sigma_z^{a_n+C_2^3}$	$\sigma_z^{a_n+C_2^4}$	$\cdots$	$\sigma_z^{a_n+C_2^{n-2}}$	$\sigma_z^{a_n+C_2^{n-1}}$	$\sigma_z^{a_n+C_2^n}$
F_{n+1}	$\Sigma_{z,y}$	$\sigma_z^{a_n+C_n^2}$	$\sigma_z^{a_n+C_n^3}$	$\sigma_z^{a_n+C_n^4}$	$\cdots$	$\sigma_z^{a_n+C_n^{n-2}}$	$\sigma_z^{a_n+C_n^{n-1}}$	$\Sigma_{x,y}$

then Eq. (31) becomes

$$F_n = \sigma_z^1 \otimes \sigma_x^2 \otimes \prod_{j=3}^{n} (\sigma_z^j)^{a_n + C_2^j}. \tag{33}$$

Case (ii). If Mod$[a_n, 2] = 1$, then one has

$$(\sigma_x)^{a_n}\sigma_z = -i\ \sigma_y, \quad (\sigma_z)^{a_n}\sigma_x = i\ \sigma_y, \tag{34}$$

then Eq. (31) becomes

$$F_n = \sigma_y^1 \otimes \sigma_y^2 \otimes \prod_{j=3}^{n} (\sigma_z^j)^{a_n + C_2^j}. \tag{35}$$

Therefore, based on Eqs. (33) and (35), we finally have F_n as

$$F_n = \Sigma_{z,y}^1 \otimes \Sigma_{x,y}^2 \otimes \prod_{j=3}^{n} (\sigma_z^j)^{a_n + C_2^j}, \tag{36}$$

with

$$\Sigma_{z,y} = \begin{cases} \sigma_z, & \text{if Mod}[a_n, 2] = 0, \\ \sigma_y, & \text{if Mod}[a_n, 2] = 1. \end{cases} \tag{37}$$

Similarly, one can make the same analysis for the operator F_{n+1}.

Base on the above analysis, we can recast the Table 2 into the form of Table 3. Now we are ready to prove the classical prediction is "+1".

In the LHV models, the observables $\sigma_{x,y,z}^i$ for the i-th qubit will be replaced by $v_{x,y,z}^i \in \{-1,+1\}$, which denote the realistic local values. For instances, we have the corresponding quantities in the LHV models as

$$\tilde{F}_1 = v_x^1 v_z^2 v_z^3 \cdots v_z^{n-1} v_z^n = v_x^1 \prod_{j=2}^{n} v_z^j, \tag{38}$$

$$\tilde{F}_2 = (v_x^1)^{a_2} V_{x,y}^2 V_{x,y}^3 (v_z^4)^{a_2+C_2^4+C_3^4} \cdots (v_z^{n-1})^{a_2+C_2^{n-1}+C_3^{n-1}} (v_z^n)^{a_2+C_2^n+C_3^n} \tag{39}$$

$$= (v_x^1)^{a_2} V_{x,y}^2 V_{x,y}^3 \prod_{j=4}^{n} (v_z^j)^{a_2+C_2^j+C_3^j}, \tag{40}$$

where

$$V_{x,y} = \begin{cases} v_x, & \text{if Mod}[a_n, 2] = 0, \\ v_y, & \text{if Mod}[a_n, 2] = 1, \end{cases} \tag{41}$$

and

$$(v^j_{x,y,z})^\ell = \begin{cases} v_{x,y,z}, & \text{if Mod}[\ell, 2] = 1, \\ 1, & \text{if Mod}[\ell, 2] = 0. \end{cases} \tag{42}$$

Similarly, for $k = 3, 4, \cdots, n-1$,

$$\tilde{F}_k = (v^1_x)^{a_k} V^k_{x,y} V^{k+1}_{x,y} \prod_{j\neq 1,k,k+1}^{n} (v^j_z)^{a_k + C^j_k + C^j_{k+1}}, \tag{43}$$

For $k = n, n+1$, one has

$$\tilde{F}_n = V^1_{z,y} V^2_{x,y} (v^3_z)^{a_n + C^3_2} (v^4_z)^{a_n + C^4_2} \cdots (v^{n-1}_z)^{a_n + C^{n-1}_2} (v^n_z)^{a_n + C^n_2} = V^1_{z,y} V^2_{x,y} \prod_{j=3}^{n} (v^j_z)^{a_n + C^j_2}, \tag{44}$$

$$\tilde{F}_{n+1} = V^1_{z,y} (v^2_z)^{a_n + C^3_n} (v^3_z)^{a_n + C^3_n} \cdots (v^{n-1}_z)^{a_n + C^{n-1}_n} V^n_{x,y} = V^1_{z,y} V^n_{x,y} \prod_{j=2}^{n-1} (v^j_z)^{a_n + C^j_n}. \tag{45}$$

Then we obtain the classical prediction as

$$\begin{aligned}
\mathcal{C} &= \prod_{k=1}^{n+1} \tilde{F}_k \\
&= \left(v^1_x \prod_{j=2}^{n} v^j_z \right) \prod_{k=2}^{n-1} \left((v^1_x)^{a_k} V^k_{x,y} V^{k+1}_{x,y} \prod_{j\neq 1,k,k+1} (v^j_z)^{a_k + C^j_k + C^j_{k+1}} \right) \left(V^1_{z,y} V^2_{x,y} \prod_{j=3}^{n} (v^j_z)^{a_n + C^j_2} \right) \left(V^1_{z,y} V^n_{x,y} \prod_{j=2}^{n-1} (v^j_z)^{a_n + C^j_n} \right) \\
&= \left[(V^1_{z,y})^2 \prod_{j=2}^{n} (V^j_{x,y})^2 \right] \times \left[(v^1_x)^{1 + \sum\limits_{k=2}^{n-1} a_k} \right] \times \left[(v^2_z)^{1 + \sum\limits_{k=3}^{n-1} (a_k + C^2_k + C^2_{k+1}) + a_n + C^2_n} \right] \\
&\quad \times \left[\prod_{j=3}^{n-1} (v^j_z)^{1 + \sum\limits_{k\neq j,j-1} (a_k + C^j_k + C^j_{k+1}) + 2a_n + C^j_2 + C^j_n} \right] \times \left[(v^n_z)^{1 + \sum\limits_{k=2}^{n-2} (a_k + C^n_k + C^n_{k+1}) + a_n + C^n_2} \right] \\
&= \left[(V^1_{z,y})^2 \prod_{j=2}^{n} (V^j_{x,y})^2 \right] (v^1_x)^{\mathcal{Z}_1} (v^2_z)^{\mathcal{Z}_2} \left[\prod_{j=3}^{n-1} (v^j_z)^{\mathcal{Z}_j} \right] (v^n_z)^{\mathcal{Z}_n} \\
&= (v^1_x)^{\mathcal{Z}_1} (v^2_z)^{\mathcal{Z}_2} \left[\prod_{j=3}^{n-1} (v^j_z)^{\mathcal{Z}_j} \right] (v^n_z)^{\mathcal{Z}_n} = \prod_{j=1}^{n} (v^j_z)^{\mathcal{Z}_j},
\end{aligned} \tag{46}$$

where in the last step of above equation, we have used the relation $(V^1_{z,y})^2 = (V^j_{x,y})^2 = 1$. Obviously, to prove the classical prediction $\mathcal{C} = +1$, one needs to prove $\mathcal{Z}_j = \textit{even number}$ for any $j \in \{1, 2, \cdots, n\}$.

From Eq. (15), we easily have

$$\mathcal{Z}_1 = 1 + \sum_{k=2}^{n-1} a_k = \text{even number}, \tag{47}$$

and

$$\begin{aligned}
\mathcal{Z}_2 &= 1 + \sum_{k=3}^{n-1} (a_k + C^2_k + C^2_{k+1}) + a_n + C^2_n \\
&= 1 + a_3 + \cdots + a_{n-1} + 2(LC^2_4 + C^2_5 + \cdots + C^2_{n-1} + C^2_n) + a_n + C^2_3 \\
&= 1 + a_3 + \cdots + a_{n-1} + 2(LC^2_4 + C^2_5 + \cdots + C^2_{n-1} + C^2_n) + (a_2 + C^2_3) + C^2_3 \\
&= 1 + \sum_{i=2}^{n-1} a_i + 2 \sum_{k=3}^{n} C^2_k \\
&= \text{even number}.
\end{aligned} \tag{48}$$

For $3 \leq j \leq n-1$, one has

$$\mathcal{Z}_j = 1 + \sum_{k \neq j, j-1} (a_k + C_k^j + C_{k+1}^j) + 2a_n + C_2^j + C_n^j, \quad (k = 2, 3, \cdots, n-1). \tag{49}$$

When $j = 3$, one obtains

$$\begin{aligned}
\mathcal{Z}_3 &= 1 + \sum_{k=4}^{n-1} (a_k + C_k^3 + C_{k+1}^3) + 2a_n + C_2^3 + C_n^3, \\
&= 1 + a_4 + a_5 + \cdots + a_{n-1} + 2a_n + 2(C_5^3 + C_6^3 + \cdots + C_{n-1}^3 + C_n^3) + LC_4^3 + C_2^3 \\
&= 1 + a_4 + a_5 + \cdots + a_{n-1} + (a_2 + C_2^3) + (a_3 + LC_4^3) + 2(C_5^3 + C_6^3 + \cdots + C_{n-1}^3 + C_n^3) + LC_4^3 + C_2^3 \\
&= 1 + \sum_{i=2}^{n-1} a_i + 2 \sum_{k=2, k\neq 3}^{n} C_k^3 \\
&= \text{even number},
\end{aligned} \tag{50}$$

Similarly, we have $\mathcal{Z}_j =$ even number, $(j = 4, 5, \cdots, n-1)$. For $j = n$, one has

$$\begin{aligned}
\mathcal{Z}_n &= 1 + \sum_{k=2}^{n-2} \left(a_k + C_k^n + C_{k+1}^n \right) + a_n + C_2^n \\
&= 1 + a_2 + \cdots + a_{n-2} + 2(C_2^n + C_3^n + \cdots + C_{n-2}^n) + a_n + C_{n-1}^n \\
&= 1 + a_2 + \cdots + a_{n-2} + 2(C_2^n + C_3^n + \cdots + C_{n-2}^n) + (a_{n-1} + C_{n-1}^n) + C_{n-1}^n \\
&= 1 + \sum_{i=2}^{n-1} a_i + 2 \sum_{k=2}^{n-1} C_k^n \\
&= \text{even number}.
\end{aligned} \tag{51}$$

In short, for $2 \leq j \leq n$, one has

$$\begin{aligned}
\mathcal{Z}_j &= 1 + \sum_{i=2}^{n-1} a_i + 2 \sum_{k=2, k\neq j}^{n} C_k^j \\
&= \text{even number}.
\end{aligned} \tag{52}$$

We finally have the classical prediction as

$$\mathcal{C} = +1. \tag{53}$$

Thus there is a sharp contradiction "$+1_{\rm C} = -1_{\rm Q}$" between the LHV models and QM. This ends the proof for GHZ-type paradox for the case of *odd* n. □

Proof. (ii) n is *even*.

Step 1.—Let us prove that quantum prediction is "-1". For simplicity, let us denote F_k as the k-th operator in the set of n operators $\{S_1,\ (-1)^{a_i} S_1^{a_i} S_i S_{i+1}\}$, i.e.,

$$F_k = [\{S_1,\ \ (-1)^{a_i} S_1^{a_i} S_i S_{i+1}\}]_k. \tag{54}$$

Based on Eq. (4), it is easy to have

$$[F_1 = S_1] |G\rangle = +1 |G\rangle, \tag{55a}$$
$$[F_i = (-1)^{a_i} S_1^{a_i} S_i S_{i+1}] |G\rangle = (-1)^{a_i} |G\rangle, \tag{55b}$$
$$(i = 2, \ldots, n). \tag{55c}$$

Then we obtain the quantum prediction as

$$\mathcal{Q} = \prod_{k=1}^{n} \langle G|F_k|G\rangle = (-1)^{\sum\limits_{i=2}^{n} a_i}. \tag{56}$$

Supplementary Table 4. The explicit forms of operators F_k, $(k = 1, 2, \cdots, n)$. Here n is *even*.

	1	2	3	4	$\cdots$	$n-2$	$n-1$	n
F_1	σ_x	σ_z	σ_z	σ_z	$\cdots$	σ_z	σ_z	σ_z
F_2	$\sigma_x^{a_2}$	$\sigma_z^{a_n+C_n^2}\sigma_x$	$\sigma_x\sigma_z^{a_n+C_n^2}$	$\sigma_z^{a_2+C_2^4+C_3^4}$	$\cdots$	$\sigma_z^{a_2+C_2^{n-2}+C_3^{n-2}}$	$\sigma_z^{a_2+C_2^{n-1}+C_3^{n-1}}$	$\sigma_z^{a_2+C_2^n+C_3^n}$
F_3	$\sigma_x^{a_3}$	$\sigma_z^{a_3+C_3^2+LC_4^2}$	$\sigma_x\sigma_z^{a_n+C_n^2}$	$\sigma_z^{a_n+C_n^2}\sigma_x$	$\cdots$	$\sigma_z^{a_3+C_3^{n-2}+LC_4^{n-2}}$	$\sigma_z^{a_3+C_3^{n-1}+LC_4^{n-1}}$	$\sigma_z^{a_3+C_3^n+LC_4^n}$
F_4	$\sigma_x^{a_4}$	$\sigma_z^{a_4+LC_4^2+C_5^2}$	$\sigma_z^{a_4+LC_4^3+C_5^3}$	$\sigma_z^{a_n+C_n^2}\sigma_x$	$\cdots$	$\sigma_z^{a_4+LC_4^{n-2}+C_5^{n-2}}$	$\sigma_z^{a_4+LC_4^{n-1}+C_5^{n-1}}$	$\sigma_z^{a_4+LC_4^n+C_5^n}$
$\vdots$	$\vdots$	$\vdots$	$\vdots$	$\vdots$	$\vdots$	$\vdots$	$\vdots$	$\vdots$
F_{n-2}	$\sigma_x^{a_{n-2}}$	$\sigma_z^{a_{n-2}+C_{n-2}^2+C_{n-1}^2}$	$\sigma_z^{a_{n-2}+C_{n-2}^3+C_{n-1}^3}$	$\sigma_z^{a_{n-2}+C_{n-2}^4+C_{n-1}^4}$	$\cdots$	$\sigma_z^{a_n+C_n^2}\sigma_x$	$\sigma_x\sigma_z^{a_n+C_n^2}$	$\sigma_z^{a_{n-2}+C_{n-2}^n+C_{n-1}^n}$
F_{n-1}	$\sigma_x^{a_{n-1}}$	$\sigma_z^{a_{n-1}+C_{n-1}^2+C_n^2}$	$\sigma_z^{a_{n-1}+C_{n-1}^3+C_n^3}$	$\sigma_z^{a_{n-1}+C_{n-1}^4+C_n^4}$	$\cdots$	$\sigma_z^{a_{n-1}+C_{n-1}^{n-2}}$	$\sigma_x\sigma_z^{a_n+C_n^2}$	$\sigma_z^{a_n+C_n^2}\sigma_x$
F_n	$\sigma_x^{a_n}$	$\sigma_z^{a_n+C_n^2}\sigma_x$	$\sigma_z^{a_n+C_n^3+C_2^3}$	$\sigma_z^{a_n+C_n^4+C_2^4}$	$\cdots$	$\sigma_z^{a_n+C_n^{n-2}+C_2^{n-2}}$	$\sigma_z^{a_n+C_n^{n-1}+C_2^{n-1}}$	$\sigma_x\sigma_z^{a_n+C_2^n}$

Because

$$\begin{aligned}\sum_{i=2}^{n} a_i &= a_2 + a_3 + a_4 + \cdots + a_n \\ &= (1 + \sum_{k\neq 2} C_k^{k+1}) + (1 + \sum_{k\neq 3} C_k^{k+1}) + (1 + \sum_{k\neq 4} C_k^{k+1}) + \cdots + (1 + \sum_{k\neq n} C_k^{k+1}) \\ &= (n-1) + (n-2)(C_2^3 + C_3^4 + C_4^5 + \cdots + C_{n-1}^n + C_n^2) \\ &= \text{odd number},\end{aligned} \tag{57}$$

thus we finally have [note that $(n-1) = odd$ and $(n-2) = even$ in the above equation]

$$\mathcal{Q} = (-1)^{\sum_{i=2}^{n} a_i} = -1. \tag{58}$$

Step 2.—Let us prove that classical prediction is "+1". In Table 4, we have listed the explicit forms for the operators F_k. For examples, for $k = 1$ we have

$$F_1 = S_1 = \sigma_x^1 \otimes \sigma_z^2 \otimes \sigma_z^3 \otimes \cdots \otimes \sigma_z^{n-1} \otimes \sigma_z^n. \tag{59}$$

For $k = 2$, we have

$$F_2 = (-1)^{a_2} S_1^{a_2} S_2 S_3 = (-1)^{a_2}\ [(\sigma_x^1)^{a_2} \otimes (\sigma_z^2)^{a_2} \sigma_x^2 (\sigma_z^2)^{C_3^2} \otimes (\sigma_z^3)^{a_2} (\sigma_z^3)^{C_2^3} \sigma_x^3 \otimes \prod_{j=4}^{n} \sigma_z^{a_2+C_2^j+C_3^j}], \tag{60}$$

according to Eq. (19) and Eq. (20), we have

$$\begin{aligned}F_2 &= (\sigma_x^1)^{a_2} \otimes \sigma_x^2 (\sigma_z^2)^{a_2+C_3^2} \otimes (\sigma_z^3)^{a_2+C_2^3} \sigma_x^3 \otimes \prod_{j=4}^{n} \sigma_z^{a_2+C_2^j+C_3^j} \\ &= (\sigma_x^1)^{a_2} \otimes (\sigma_z^2)^{a_2+C_3^2} \sigma_x^2 \otimes \sigma_x^3 (\sigma_z^3)^{a_2+C_2^3} \otimes \prod_{j=4}^{n} \sigma_z^{a_2+C_2^j+C_3^j},\end{aligned} \tag{61}$$

From Eq. (10), one has

$$a_i + C_i^{i+1} = a_n + C_n^2, \tag{62}$$

then, Eq. (61) becomes

$$F_2 = (\sigma_x^1)^{a_2} \otimes (\sigma_z^2)^{a_n+C_n^2} \sigma_x^2 \otimes \sigma_x^3 (\sigma_z^3)^{a_n+C_n^2} \otimes \prod_{j=4}^{n} \sigma_z^{a_2+C_2^j+C_3^j}. \tag{63}$$

Supplementary Table 5. Another explicit forms of operators F_k, $(k=1,2,\cdots,n)$. Here n is *even*.

	1	2	3	4	$\cdots$	$n-2$	$n-1$	n
F_1	σ_x	σ_z	σ_z	σ_z	$\cdots$	σ_z	σ_z	σ_z
F_2	$\sigma_x^{a_2}$	$\Sigma_{x,y}$	$\Sigma_{x,y}$	$\sigma_z^{a_2+C_2^4+C_3^4}$	$\cdots$	$\sigma_z^{a_2+C_2^{n-2}+C_3^{n-2}}$	$\sigma_z^{a_2+C_2^{n-1}+C_3^{n-1}}$	$\sigma_z^{a_2+C_2^n+C_3^n}$
F_3	$\sigma_x^{a_3}$	$\sigma_z^{a_3+C_3^2+LC_4^2}$	$\Sigma_{x,y}$	$\Sigma_{x,y}$	$\cdots$	$\sigma_z^{a_3+C_3^{n-2}+LC_4^{n-2}}$	$\sigma_z^{a_3+C_3^{n-1}+LC_4^{n-1}}$	$\sigma_z^{a_3+C_3^n+LC_4^n}$
F_4	$\sigma_x^{a_4}$	$\sigma_z^{a_4+LC_4^2+C_5^2}$	$\sigma_z^{a_4+LC_4^3+C_5^3}$	$\Sigma_{x,y}$	$\cdots$	$\sigma_z^{a_4+LC_4^{n-2}+C_5^{n-2}}$	$\sigma_z^{a_4+LC_4^{n-1}+C_5^{n-1}}$	$\sigma_z^{a_4+LC_4^n+C_5^n}$
$\vdots$	$\vdots$	$\vdots$	$\vdots$	$\vdots$	$\vdots$	$\vdots$	$\vdots$	$\vdots$
F_{n-2}	$\sigma_x^{a_{n-2}}$	$\sigma_z^{a_{n-2}+C_{n-2}^2+C_{n-1}^2}$	$\sigma_z^{a_{n-2}+C_{n-2}^3+C_{n-1}^3}$	$\sigma_z^{a_{n-2}+C_{n-2}^4+C_{n-1}^4}$	$\cdots$	$\Sigma_{x,y}$	$\Sigma_{x,y}$	$\sigma_z^{a_{n-2}+C_{n-2}^n+C_{n-1}^n}$
F_{n-1}	$\sigma_x^{a_{n-1}}$	$\sigma_z^{a_{n-1}+C_{n-1}^2+C_n^2}$	$\sigma_z^{a_{n-1}+C_{n-1}^3+C_n^3}$	$\sigma_z^{a_{n-1}+C_{n-1}^4+C_n^4}$	$\cdots$	$\sigma_z^{a_{n-1}+C_{n-1}^{n-2}}$	$\Sigma_{x,y}$	$\Sigma_{x,y}$
F_n	$\sigma_x^{a_n}$	$\Sigma_{x,y}$	$\sigma_z^{a_n+C_n^3+C_2^3}$	$\sigma_z^{a_n+C_n^4+C_2^4}$	$\cdots$	$\sigma_z^{a_n+C_n^{n-2}+C_2^{n-2}}$	$\sigma_z^{a_n+C_n^{n-1}+C_2^{n-1}}$	$\Sigma_{x,y}$

which is just the one listed in Table 4. Similarly, one can directly calculate other F_k's $(k=3,4,\cdots,n)$, their explicit forms are given in Table 4.

Remark 3.—For $k=2$. Case (i) If $\text{Mod}[a_n+C_n^2,2]=0$, one has

$$(\sigma_z)^{a_n+C_n^2}\sigma_x=\sigma_x,\quad \sigma_x(\sigma_z)^{a_n+C_n^2}=\sigma_x, \tag{64}$$

then F_2 can be written as

$$F_2=(\sigma_x^1)^{a_2}\otimes\sigma_x^2\otimes\sigma_x^3\otimes\prod_{j=4}^{n}\sigma_z^{a_2+C_2^j+C_3^j}. \tag{65}$$

Case (ii). If $\text{Mod}[a_n+C_n^2,2]=1$, one has

$$(\sigma_z)^{a_n+C_n^2}\sigma_x=i\ \sigma_y,\quad \sigma_x(\sigma_z)^{a_n+C_n^2}=-i\ \sigma_y, \tag{66}$$

then F_2 can be written as

$$F_2=(\sigma_x^1)^{a_2}\otimes\sigma_y^2\otimes\sigma_y^3\otimes\prod_{j=4}^{n}\sigma_z^{a_2+C_2^j+C_3^j}. \tag{67}$$

Finally, one obtains

$$F_2=(\sigma_x^1)^{a_2}\otimes\Sigma_{x,y}^2\otimes\Sigma_{x,y}^3\otimes\prod_{j=4}^{n}\sigma_z^{a_2+C_2^j+C_3^j}. \tag{68}$$

with

$$\Sigma_{x,y}=\begin{cases}\sigma_x, & \text{if } \text{Mod}[a_n+C_n^2,2]=0,\\ \sigma_y, & \text{if } \text{Mod}[a_n+C_n^2,2]=1.\end{cases} \tag{69}$$

Similarly, one can make the same analysis for other F_k's, with $k=3,4,\cdots,n$.

Base on the above analysis, we can recast the Table 4 into the form of Table 5. Now we are ready to prove the classical prediction is "+1". When n is even, we have have the corresponding quantities in the LHV models as

$$\tilde{F}_1=v_x^1v_z^2v_z^3\cdots v_z^{n-1}v_z^n=v_x^1\prod_{j=2}^{n}v_z^j, \tag{70}$$

$$\tilde{F}_k=(v_x^1)^{a_k}V_{x,y}^kV_{x,y}^{k+1}\prod_{j\neq k,k+1}^{n}(v_z^j)^{a_k+C_k^j+C_{k+1}^j},\quad (k=2,3,\cdots,n-1,\ \ j=2,3,\cdots,n), \tag{71}$$

$$\begin{aligned}\tilde{F}_n &= (v_x^1)^{a_n} V_{x,y}^2 (v_z^3)^{a_n+C_n^3+C_2^3} (v_z^4)^{a_n+C_n^4+C_2^4} \cdots (v_z^{n-1})^{a_n+C_n^{n-1}+C_2^{n-1}} V_{x,y}^n \\ &= (v_x^1)^{a_n} V_{x,y}^2 V_{x,y}^n \prod_{j=3}^{n-1} (v_z^j)^{a_n+C_n^j+C_2^j}. \end{aligned} \tag{72}$$

Then we obtain the classical prediction as

$$\begin{aligned}\mathcal{C} &= \prod_{k=1}^{n} \tilde{F}_k \\ &= \left(v_x^1 \prod_{j=2}^{n} v_z^j\right) \prod_{k=2}^{n-1} \left((v_x^1)^{a_k} V_{x,y}^k V_{x,y}^{k+1} \prod_{j\neq k,k+1} (v_z^j)^{a_k+C_k^j+C_{k+1}^j}\right) \left((v_x^1)^{a_n} V_{x,y}^2 V_{x,y}^n \prod_{j=3}^{n-1} (v_z^j)^{a_n+C_n^j+C_2^j}\right) \\ &= \prod_{j=2}^{n} (V_{x,y}^j)^2 (v_x^1)^{1+\sum_{k=2}^{n} a_k} (v_z^2)^{1+\sum_{k=3}^{n-1}(a_k+C_k^2+C_{k+1}^2)} \prod_{j=3}^{n} (v_z^j)^{1+\sum_{k\neq j,j-1}(a_k+C_k^j+C_{k+1}^j)} \\ &= (v_x^1)^{1+\sum_{k=2}^{n} a_k} (v_z^2)^{1+\sum_{k=3}^{n-1}(a_k+C_k^2+C_{k+1}^2)} \prod_{j=3}^{n} (v_z^j)^{1+\sum_{k\neq j,j-1}(a_k+C_k^j+C_{k+1}^j)} \\ &= \prod_{j=1}^{n} (v_z^j)^{\mathcal{Z}_j}, \end{aligned} \tag{73}$$

here $C_{n+1}^i = C_2^i$. Similarly, to prove the classical prediction $\mathcal{C} = +1$, one needs to prove $\mathcal{Z}_j = \textit{even number}$ for any $j \in \{1, 2, \cdots, n\}$.

From Eq. (57), we immediately have

$$\mathcal{Z}_1 = 1 + \sum_{k=2}^{n} a_k = \text{even number}. \tag{74}$$

For $j = 2$, we have

$$\begin{aligned}\mathcal{Z}_2 &= 1 + \sum_{k=3}^{n-1} (a_k + C_k^2 + C_{k+1}^2) \\ &= 1 + (a_3 + \cdots + a_{n-1}) + 2(C_4^2 + C_5^2 + \cdots + C_{n-1}^2) + C_3^2 + C_n^2 \\ &= 1 + \sum_{i=2}^{n} a_i + 2(C_3^2 + C_4^2 + \cdots + C_{n-1}^2) + [-a_2 - a_n - C_3^2 + C_n^2] \\ &= 1 + \sum_{i=2}^{n} a_i + 2(C_3^2 + C_4^2 + \cdots + C_{n-1}^2 - a_n) \\ &= \text{even number}, \end{aligned} \tag{75}$$

Here we have used

$$a_2 + C_3^2 = a_n + C_n^2. \tag{76}$$

For $3 \leq j \leq n$, one has

$$\mathcal{Z}_j = 1 + \sum_{k\neq j,j-1} (a_k + C_k^j + C_{k+1}^j), \quad (k = 2, 3, \cdots, n). \tag{77}$$

When $j=3$,

$$\begin{aligned}
\mathcal{Z}_3 &= 1+\sum_{k=4}^{n}(a_k+C_k^3+C_{k+1}^3),\\
&= 1+a_4+\cdots+a_n+2(C_5^3+\cdots+C_n^3)+C_4^3+C_2^3\\
&= 1+\sum_{i=2}^{n}a_i+2(C_5^3+\cdots+C_n^3)+(-a_2-a_3+C_4^3+C_2^3) \qquad (78)\\
&= 1+\sum_{i=2}^{n}a_i+2(LC_4^3+C_5^3+\cdots+C_n^3-a_2) \qquad (79)\\
&= \text{even number}, \qquad (80)
\end{aligned}$$

Here we have used

$$a_2+C_2^3=a_3+C_3^4. \tag{81}$$

similarly, $\mathcal{Z}_j=$ even number, $j=4,5,\cdots,n$. Thus we finally have

$$\mathcal{C}=+1. \tag{82}$$

Thus there is a sharp contradiction "$+1_{\rm C}=-1_{\rm Q}$" between the LHV models and QM. This ends the proof for GHZ-type paradox for the case of *odd* n. □

B. Some examples for Theorem 1

For the cases of $m=3$ and 4, in Fig. 1, we have listed all the possible and nontrivial graphs. In the following, we list the corresponding GHZ-type paradox for each graph.

Example 1.—For the graph as Fig. 1(a), we have $m=n=3$. The corresponding ground state of the Hamiltonian $\mathcal{H}$ is $|G\rangle=(|000\rangle+|001\rangle+|010\rangle+|011\rangle+|100\rangle-|101\rangle-|110\rangle+|111\rangle)/2\sqrt{2}$. From Theorem 1, we have $\{a_2=1,a_3=1\}$, then the GHZ-type paradox "$+1_{\rm C}=-1_{\rm Q}$" can be arisen from the following 4 operators:

$$S_1=\sigma_x^1\sigma_z^2\sigma_z^3, \tag{83a}$$
$$-S_1S_2S_3=\sigma_x^1\sigma_y^2\sigma_y^3, \tag{83b}$$
$$S_1S_3=\sigma_y^1\sigma_z^2\sigma_y^3, \tag{83c}$$
$$S_1S_2=\sigma_y^1\sigma_y^2\sigma_z^3, \tag{83d}$$

i.e., $S_1|G\rangle=+|G\rangle$, $-S_1S_2S_3|G\rangle=-|G\rangle$, $S_1S_3|G\rangle=+|G\rangle$, $S_1S_2|G\rangle=+|G\rangle$.

Through the unitary transformation $\mathcal{U}=\mathbb{1}\otimes U_1\otimes U_1$, with $U_1=(\sigma_x+\sigma_z)/\sqrt{2}$, the state $|G\rangle$ is equivalent to the 3-qubit GHZ state $|GHZ_3\rangle=(|000\rangle+|111\rangle)/\sqrt{2}$, and the 4 operators become

$$E_1=\sigma_x^1\sigma_x^2\sigma_x^3, \tag{84a}$$
$$E_2=\sigma_x^1\sigma_y^2\sigma_y^3, \tag{84b}$$
$$E_3=\sigma_y^1\sigma_x^2\sigma_y^3, \tag{84c}$$
$$E_4=\sigma_y^1\sigma_y^2\sigma_x^3. \tag{84d}$$

It can be constructed the original 3-qubit GHZ paradox:

$$\sigma_x^1\sigma_x^2\sigma_x^3|GHZ_3\rangle=+|GHZ_3\rangle, \tag{85a}$$
$$\sigma_x^1\sigma_y^2\sigma_y^3|GHZ_3\rangle=-|GHZ_3\rangle, \tag{85b}$$
$$\sigma_y^1\sigma_x^2\sigma_y^3|GHZ_3\rangle=-|GHZ_3\rangle, \tag{85c}$$
$$\sigma_y^1\sigma_y^2\sigma_x^3|GHZ_3\rangle=-|GHZ_3\rangle. \tag{85d}$$

In the LHV models, σ_i are assumed to have definite values $v_i=\pm1$ even before the measurements, it follows that

$$v_x^1v_x^2v_x^3=+1, \tag{86a}$$
$$v_x^1v_y^2v_y^3=-1, \tag{86b}$$
$$v_y^1v_x^2v_y^3=-1, \tag{86c}$$
$$v_y^1v_y^2v_x^3=-1, \tag{86d}$$

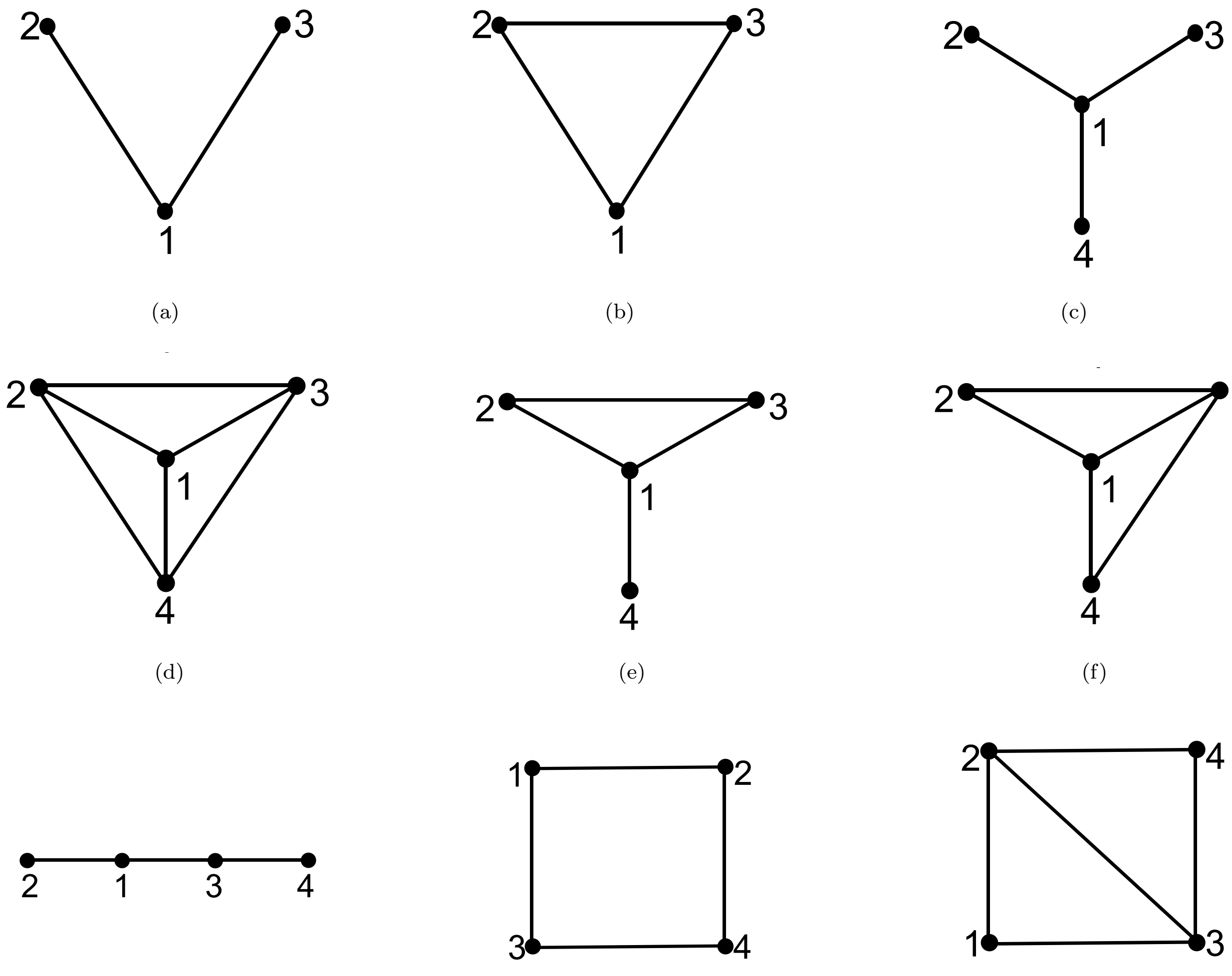

(a) (b) (c) (d) (e) (f) (g) (h) (i)

Supplementary Figure 1. The graphs for $m = 3, 4$. Graphs (a) and (b) correspond to the scenario $(m, n) = (3, 3)$, and their corresponding ground states are given by the 3-qubit GHZ state $|G\rangle \equiv |GHZ_3\rangle = (|000\rangle + |111\rangle)/\sqrt{2}$ up to a local unitary transformation (LUT). Graphs (c) and (d) correspond to the scenario $(m, n) = (4, 4)$, and their corresponding ground states are the 4-qubit GHZ state $|G\rangle \equiv |GHZ_4\rangle = (|0000\rangle + |1111\rangle)/\sqrt{2}$ up to a LUT. Graphs (e) and (f) correspond to the scenario $(m, n) = (4, 4)$, graphs (g), (h) and (i) correspond to the scenario $(m, n) = (4, 3)$, and the corresponding ground states are given by the 4-qubit cluster state $|G\rangle \equiv |LC_4\rangle = (|0000\rangle + |0011\rangle + |1100\rangle - |1111\rangle)/2$ up to a LUT.

When one multiplies the above four equations, the left-hand side gives the classical prediction as

$$\mathcal{C} = (v_x^1)^2 (v_y^1)^2 (v_x^2)^2 (v_y^2)^2 (v_x^3)^2 (v_y^3)^2 = +1, \tag{87}$$

but the right-hand side gives the quantum prediction as $\mathcal{Q} = -1$, thus leads to the sharp contradiction of "$+1_{\rm C} = -1_{\rm Q}$".

Example 2.—For the graph as Fig. 1(b), we have $m = n = 3$. The ground state is $|G\rangle = (|000\rangle + |001\rangle + |010\rangle - |011\rangle + |100\rangle - |101\rangle - |110\rangle - |111\rangle)/(2\sqrt{2})$. From Theorem 1, we have $\{a_2 = 1, a_3 = 2\}$, then the GHZ-type paradox can be arisen from the following 4 operators:

$$S_1 = \sigma_x^1 \sigma_z^2 \sigma_z^3, \tag{88a}$$
$$-S_1 S_2 S_3 = \sigma_x^1 \sigma_x^2 \sigma_x^3, \tag{88b}$$
$$S_3 = \sigma_z^1 \sigma_z^2 \sigma_x^3, \tag{88c}$$
$$S_2 = \sigma_z^1 \sigma_x^2 \sigma_z^3, \tag{88d}$$

i.e., $S_1|G\rangle = +|G\rangle$, $-S_1 S_2 S_3|G\rangle = -|G\rangle$, $S_3|G\rangle = +|G\rangle$, $S_2|G\rangle = +|G\rangle$.

Through the unitary transformation $\mathcal{U} = U_1 \otimes U_1 \otimes U_1$, with $U_1 = (\sigma_y + \sigma_z)/\sqrt{2}$, the state $|G\rangle$ is equivalent to the 3-qubit GHZ state $|GHZ_3\rangle = (|000\rangle + |111\rangle)/\sqrt{2}$, and the 4 operators become

$$E_1 = \sigma_x^1\sigma_y^2\sigma_y^3, \tag{89a}$$
$$E_2 = \sigma_x^1\sigma_x^2\sigma_x^3, \tag{89b}$$
$$E_3 = \sigma_y^1\sigma_y^2\sigma_x^3, \tag{89c}$$
$$E_4 = \sigma_y^1\sigma_x^2\sigma_y^3. \tag{89d}$$

It can be constructed the original 3-qubit GHZ paradox:

$$\sigma_x^1\sigma_y^2\sigma_y^3|GHZ_3\rangle = -|GHZ_3\rangle, \tag{90a}$$
$$\sigma_x^1\sigma_x^2\sigma_x^3|GHZ_3\rangle = +|GHZ_3\rangle, \tag{90b}$$
$$\sigma_y^1\sigma_y^2\sigma_x^3|GHZ_3\rangle = -|GHZ_3\rangle, \tag{90c}$$
$$\sigma_y^1\sigma_x^2\sigma_y^3|GHZ_3\rangle = -|GHZ_3\rangle. \tag{90d}$$

In LHV models, σ_i are assumed to have definite values $v_i = \pm 1$, it follows that

$$v_x^1 v_y^2 v_y^3 = -1, \tag{91a}$$
$$v_x^1 v_x^2 v_x^3 = +1, \tag{91b}$$
$$v_y^1 v_y^2 v_x^3 = -1, \tag{91c}$$
$$v_y^1 v_x^2 v_y^3 = -1, \tag{91d}$$

When one multiplies the above four equations, the left-hand side gives $(v_x^1)^2(v_y^1)^2(v_x^2)^2(v_y^2)^2(v_x^3)^2(v_y^3)^2 = +1$, but the right-hand side gives the quantum prediction as -1, thus leads to the sharp contradiction of "$+1_{\rm C} = -1_{\rm Q}$".

Example 3.—For the graph as Fig. 1(c), $m = n = 4$. The ground state is $|G\rangle = (1/4)(1,1,1,1,1,1,1,1,1,-1,-1,1,-1,1,1,-1)^T$, where T means transpose. From Theorem 1, we have $\{a_2 = 1, a_3 = 1, a_4 = 1\}$, then the GHZ-type paradox can be arisen from the following 4 operators:

$$S_1 = \sigma_x^1\sigma_z^2\sigma_z^3\sigma_z^4, \tag{92a}$$
$$-S_1S_2S_3 = \sigma_x^1\sigma_y^2\sigma_y^3\sigma_z^4, \tag{92b}$$
$$-S_1S_3S_4 = \sigma_x^1\sigma_z^2\sigma_y^3\sigma_y^4, \tag{92c}$$
$$-S_1S_4S_2 = \sigma_x^1\sigma_y^2\sigma_z^3\sigma_y^4, \tag{92d}$$

i.e., $S_1|G\rangle = +|G\rangle$, $-S_1S_2S_3|G\rangle = -|G\rangle$, $-S_1S_3S_4|G\rangle = -|G\rangle$, $-S_1S_4S_2|G\rangle = -|G\rangle$.

Through the unitary transformation $\mathcal{U} = \mathbb{1} \otimes U_1 \otimes U_1 \otimes U_1$, with $U_1 = (\sigma_x + \sigma_z)/\sqrt{2}$, the state $|G\rangle$ is equivalent to the 4-qubit GHZ state $|GHZ_4\rangle = (|0000\rangle + |1111\rangle)/\sqrt{2}$, and the 4 operators become

$$E_1 = \sigma_x^1\sigma_x^2\sigma_x^3\sigma_x^4, \tag{93a}$$
$$E_2 = \sigma_x^1\sigma_y^2\sigma_y^3\sigma_x^4, \tag{93b}$$
$$E_3 = \sigma_x^1\sigma_x^2\sigma_y^3\sigma_y^4, \tag{93c}$$
$$E_4 = \sigma_x^1\sigma_y^2\sigma_x^3\sigma_y^4. \tag{93d}$$

It can be constructed the 4-qubit GHZ paradox:

$$\sigma_x^1\sigma_x^2\sigma_x^3\sigma_x^4|GHZ_4\rangle = +|GHZ_4\rangle, \tag{94a}$$
$$\sigma_x^1\sigma_y^2\sigma_y^3\sigma_x^4|GHZ_4\rangle = -|GHZ_4\rangle, \tag{94b}$$
$$\sigma_x^1\sigma_x^2\sigma_y^3\sigma_y^4|GHZ_4\rangle = -|GHZ_4\rangle, \tag{94c}$$
$$\sigma_x^1\sigma_y^2\sigma_x^3\sigma_y^4|GHZ_4\rangle = -|GHZ_4\rangle. \tag{94d}$$

In LHV models, σ_i are assumed to have definite values $v_i = \pm 1$, it follows that

$$v_x^1 v_x^2 v_x^3 v_x^4 = +1, \tag{95a}$$
$$v_x^1 v_y^2 v_y^3 v_x^4 = -1, \tag{95b}$$
$$v_x^1 v_x^2 v_y^3 v_y^4 = -1, \tag{95c}$$
$$v_x^1 v_y^2 v_x^3 v_y^4 = -1. \tag{95d}$$

When one multiplies the above four equations, the left-hand side gives $(v_x^1)^4(v_x^2)^2(v_y^2)^2(v_x^3)^2(v_y^3)^2(v_x^4)^2(v_y^4)^2 = +1$, but the right-hand side gives the quantum prediction as -1, thus leads to the sharp contradiction of "$+1_{\rm C} = -1_{\rm Q}$".

Example 4.—For the graph as Fig. 1(d), $m = n = 4$. The ground state is $|G\rangle = (1/4)(1, 1, 1, -1, 1, -1, -1, -1, 1, -1, -1, -1, -1, -1, -1, 1)^T$. From Theorem 1, we have $\{a_2 = 3, a_3 = 3, a_4 = 3\}$, then the GHZ-type paradox can be arisen from the following 4 operators:

$$S_1 = \sigma_x^1\sigma_z^2\sigma_z^3\sigma_z^4, \tag{96a}$$
$$-S_1S_2S_3 = \sigma_x^1\sigma_x^2\sigma_x^3\sigma_z^4, \tag{96b}$$
$$-S_1S_3S_4 = \sigma_x^1\sigma_z^2\sigma_x^3\sigma_x^4, \tag{96c}$$
$$-S_1S_4S_2 = \sigma_x^1\sigma_x^2\sigma_z^3\sigma_x^4, \tag{96d}$$

i.e., $S_1|G\rangle = +|G\rangle$, $-S_1S_2S_3|G\rangle = -|G\rangle$, $-S_1S_3S_4|G\rangle = -|G\rangle$, $-S_1S_4S_2|G\rangle = -|G\rangle$.

Through the unitary transformation $\mathcal{U} = U_1\otimes U_2\otimes U_2\otimes U_2$, with $U_1 = (-i\sigma_y + i\sigma_z)/\sqrt{2}, U_2 = (\mathbb{1} + i\sigma_x + i\sigma_y - i\sigma_z)/2$, the state $|G\rangle$ is equivalent to the state $|GHZ_4\rangle$, and the 4 operator become

$$E_1 = \sigma_x^1\sigma_x^2\sigma_x^3\sigma_x^4, \tag{97a}$$
$$E_2 = \sigma_x^1\sigma_y^2\sigma_y^3\sigma_x^4, \tag{97b}$$
$$E_3 = \sigma_x^1\sigma_x^2\sigma_y^3\sigma_y^4, \tag{97c}$$
$$E_4 = \sigma_x^1\sigma_y^2\sigma_x^3\sigma_y^4. \tag{97d}$$

It can be constructed the 4-qubit GHZ paradox:

$$\sigma_x^1\sigma_x^2\sigma_x^3\sigma_x^4|GHZ_4\rangle = +|GHZ_4\rangle, \tag{98a}$$
$$\sigma_x^1\sigma_y^2\sigma_y^3\sigma_x^4|GHZ_4\rangle = -|GHZ_4\rangle, \tag{98b}$$
$$\sigma_x^1\sigma_x^2\sigma_y^3\sigma_y^4|GHZ_4\rangle = -|GHZ_4\rangle, \tag{98c}$$
$$\sigma_x^1\sigma_y^2\sigma_x^3\sigma_y^4|GHZ_4\rangle = -|GHZ_4\rangle. \tag{98d}$$

In LHV models, σ_i are assumed to have definite values $v_i = \pm 1$, it follows that

$$v_x^1v_x^2v_x^3v_x^4 = +1, \tag{99a}$$
$$v_x^1v_y^2v_y^3v_x^4 = -1, \tag{99b}$$
$$v_x^1v_x^2v_y^3v_y^4 = -1, \tag{99c}$$
$$v_x^1v_y^2v_x^3v_y^4 = -1, \tag{99d}$$

when one multiplies the above four equations, the left-hand side gives $(v_x^1)^4(v_x^2)^2(v_y^2)^2(v_x^3)^2(v_y^3)^2(v_x^4)^2(v_y^4)^2 = +1$, but the right-hand side gives -1, thus leads to the sharp contradiction of "$+1_{\rm C} = -1_{\rm Q}$".

Example 5.—For the graph as Fig. 1(e), $m = n = 4$. The ground state is $|G\rangle = (1/4)(1, 1, 1, 1, 1, 1, -1, -1, 1, -1, -1, 1, -1, 1, -1, 1)^T$. From Theorem 1, we have $\{a_2 = 1, a_3 = 2, a_4 = 2\}$, then the GHZ-type paradox can be arisen from the following 4 operators:

$$S_1 = \sigma_x^1\sigma_z^2\sigma_z^3\sigma_z^4, \tag{100a}$$
$$-S_1S_2S_3 = \sigma_x^1\sigma_x^2\sigma_x^3\sigma_z^4, \tag{100b}$$
$$S_3S_4 = \mathbb{1}\sigma_z^2\sigma_x^3\sigma_x^4, \tag{100c}$$
$$S_4S_2 = \mathbb{1}\sigma_x^2\sigma_z^3\sigma_x^4, \tag{100d}$$

i.e., $S_1|G\rangle = +|G\rangle$, $-S_1S_2S_3|G\rangle = -|G\rangle$, $S_3S_4|G\rangle = +|G\rangle$, $S_4S_2|G\rangle = +|G\rangle$.

Through the unitary transformation $\mathcal{U} = \mathbb{1}\otimes U_1\otimes U_2\otimes U_3$, with $U_1 = (-\sigma_y + \sigma_z)/\sqrt{2}, U_2 = (\mathbb{1} + i\sigma_x + i\sigma_y - i\sigma_z)/2, U_3 = (\mathbb{1} + i\sigma_x + i\sigma_y + i\sigma_z)/2$, the state $|G\rangle$ is equivalent to the 4-qubit cluster state in the form $|CL_4\rangle = (|0000\rangle + |0110\rangle + |1001\rangle - |1111\rangle)/2$ (Notice: the state $|CL_4\rangle$ is equivalent to the standard form of 4-qubit cluster state $|LC_4\rangle = (|0000\rangle + |0011\rangle + |1100\rangle - |1111\rangle)/2$ by exchange the qubits 2 and 4), and the 4 operators become

$$E_1 = \sigma_x^1\sigma_y^2\sigma_x^3\sigma_y^4, \tag{101a}$$
$$E_2 = \sigma_x^1\sigma_x^2\sigma_y^3\sigma_y^4, \tag{101b}$$
$$E_3 = \mathbb{1}\sigma_y^2\sigma_y^3\sigma_z^4, \tag{101c}$$
$$E_4 = \mathbb{1}\sigma_x^2\sigma_x^3\sigma_z^4. \tag{101d}$$

It can be constructed the 4-qubit GHZ-type paradox:

$$\sigma_x^1\sigma_y^2\sigma_x^3\sigma_y^4|CL_4\rangle = +|CL_4\rangle, \tag{102a}$$
$$\sigma_x^1\sigma_x^2\sigma_y^3\sigma_y^4|CL_4\rangle = +|CL_4\rangle, \tag{102b}$$
$$\mathbb{1}\sigma_y^2\sigma_y^3\sigma_z^4|CL_4\rangle = -|CL_4\rangle, \tag{102c}$$
$$\mathbb{1}\sigma_x^2\sigma_x^3\sigma_z^4|CL_4\rangle = +|CL_4\rangle. \tag{102d}$$

In LHV models, σ_i are assumed to have definite values $v_i = \pm 1$, it follows that

$$v_x^1 v_y^2 v_x^3 v_y^4 = +1, \tag{103a}$$
$$v_x^1 v_x^2 v_y^3 v_y^4 = +1, \tag{103b}$$
$$v_y^2 v_y^3 v_z^4 = -1, \tag{103c}$$
$$v_x^2 v_x^3 v_z^4 = +1. \tag{103d}$$

When one multiplies the above four equations, the left-hand side gives $(v_x^1)^2(v_x^2)^2(v_y^2)^2(v_x^3)^2(v_y^3)^2(v_y^4)^2(v_z^4)^2 = +1$, but the right-hand side gives the quantum prediction as -1, thus leads to the sharp contradiction of "$+1_{\rm C} = -1_{\rm Q}$".

Example 6.—For the graph as Fig. 1(f), $m = n = 4$. The ground state is $|G\rangle = (1/4)(1, 1, 1, -1, 1, 1, -1, 1, 1, -1, -1, -1, -1, 1, -1, -1)^T$. From Theorem 1, we have $\{a_2 = 2, a_3 = 2, a_4 = 3\}$, then the GHZ-type paradox can be arisen from the following 4 operators:

$$S_1 = \sigma_x^1\sigma_z^2\sigma_z^3\sigma_z^4, \tag{104a}$$
$$S_2S_3 = \mathbb{1}\sigma_y^2\sigma_y^3\sigma_z^4, \tag{104b}$$
$$S_3S_4 = \mathbb{1}\sigma_z^2\sigma_y^3\sigma_y^4, \tag{104c}$$
$$-S_1S_4S_2 = \sigma_x^1\sigma_y^2\sigma_z^3\sigma_y^4, \tag{104d}$$

i.e., $S_1|G\rangle = +|G\rangle$, $S_2S_3|G\rangle = +|G\rangle$, $S_3S_4|G\rangle = +|G\rangle$, $-S_1S_4S_2|G\rangle = -|G\rangle$.

Through the unitary transformation $\mathcal{U} = \otimes U_1 \otimes U_2 \otimes U_1 \otimes U_3$, with $U_1 = (\mathbb{1}+i\sigma_x+i\sigma_y-i\sigma_z)/2, U_2 = (\mathbb{1}-i\sigma_x+i\sigma_y-i\sigma_z)/2, U_3 = (\sigma_x+\sigma_z)/\sqrt{2}$, the state $|G\rangle$ is equivalent to the state $|CL_4'\rangle = (|0000\rangle+|0101\rangle+|1010\rangle-|1111\rangle)/2$ (Notice: the state $|CL_4'\rangle$ is equivalent to the standard form of 4-qubit cluster state $|LC_4\rangle = (|0000\rangle+|0011\rangle+|1100\rangle-|1111\rangle)/2$ by exchange the qubits 2 and 3), and the 4 operators become

$$E_1 = \sigma_y^1\sigma_y^2\sigma_x^3\sigma_x^4, \tag{105a}$$
$$E_2 = \mathbb{1}\sigma_x^2\sigma_z^3\sigma_x^4, \tag{105b}$$
$$E_3 = \mathbb{1}\sigma_y^2\sigma_z^3\sigma_y^4, \tag{105c}$$
$$E_4 = \sigma_y^1\sigma_x^2\sigma_x^3\sigma_y^4. \tag{105d}$$

It can be constructed the 4-qubit GHZ-type paradox:

$$\sigma_y^1\sigma_y^2\sigma_x^3\sigma_x^4|CL_4'\rangle = +|CL_4'\rangle, \tag{106a}$$
$$\mathbb{1}\sigma_x^2\sigma_z^3\sigma_x^4|CL_4'\rangle = +|CL_4'\rangle, \tag{106b}$$
$$\mathbb{1}\sigma_y^2\sigma_z^3\sigma_y^4|CL_4'\rangle = -|CL_4'\rangle, \tag{106c}$$
$$\sigma_y^1\sigma_x^2\sigma_x^3\sigma_y^4|CL_4'\rangle = +|CL_4'\rangle. \tag{106d}$$

In LHV models, σ_i are assumed to have definite values $v_i = \pm 1$, it follows that

$$v_y^1 v_y^2 v_x^3 v_x^4 = +1, \tag{107a}$$
$$v_x^2 v_z^3 v_x^4 = +1, \tag{107b}$$
$$v_y^2 v_z^3 v_y^4 = -1, \tag{107c}$$
$$v_y^1 v_x^2 v_x^3 v_y^4 = +1. \tag{107d}$$

When one multiplies the above four equations, the left-hand side gives $(v_y^1)^2(v_x^2)^2(v_y^2)^2(v_x^3)^2(v_z^3)^2(v_x^4)^2(v_y^4)^2 = +1$, but the right-hand side gives the quantum prediction as -1, thus leads to the sharp contradiction of "$+1_{\rm C} = -1_{\rm Q}$".

Example 7.—For the graph as Fig. 1(g), $m = 4, n = 3$. The ground state is the 4-qubit cluster state in the form $|G\rangle = (|0++0\rangle + |0+-1\rangle + |1--0\rangle + |1-+1\rangle)/2$, where $|\pm\rangle = (|0\rangle \pm |1\rangle)/\sqrt{2}$. We consider the vertex 1 and its link vertices $2,3$. From Theorem 1, we have $\{a_2=1, a_3=1\}$, then the GHZ-type paradox can be arisen from the following 4 operators:

$$S_1=\sigma_x^1\sigma_z^2\sigma_z^3\mathbb{1}, \tag{108a}$$
$$-S_1S_2S_3=\sigma_x^1\sigma_y^2\sigma_y^3\sigma_z^4, \tag{108b}$$
$$S_1S_2=\sigma_y^1\sigma_y^2\sigma_z^3\mathbb{1}, \tag{108c}$$
$$S_1S_3=\sigma_y^1\sigma_z^2\sigma_y^3\sigma_z^4, \tag{108d}$$

i.e., $S_1|G\rangle=+|G\rangle$, $-S_1S_2S_3|G\rangle=-|G\rangle$, $S_1S_2|G\rangle=+|G\rangle$, $S_1S_3|G\rangle=+|G\rangle$.

Through the unitary transformation $\mathcal{U}=U_1\otimes U_2\otimes\mathbb{1}\otimes U_3$, with $U_1=\sigma_z, U_2=(\mathbb{1}+i\sigma_y)/\sqrt{2}, U_3=(\sigma_x+\sigma_z)/\sqrt{2}$, then the state $|G\rangle$ is equivalent to the standard 4-qubit cluster state $|LC_4\rangle=(|0000\rangle+|0011\rangle+|1100\rangle-|1111\rangle)/2$, and the 4 operators become

$$E_1=\sigma_x^1\sigma_x^2\sigma_z^3\mathbb{1}, \tag{109a}$$
$$E_2=\sigma_x^1\sigma_y^2\sigma_y^3\sigma_x^4, \tag{109b}$$
$$E_3=\sigma_y^1\sigma_y^2\sigma_z^3\mathbb{1}, \tag{109c}$$
$$E_4=\sigma_y^1\sigma_x^2\sigma_y^3\sigma_x^4. \tag{109d}$$

It can be constructed the 4-qubit GHZ paradox:

$$\sigma_x^1\sigma_x^2\sigma_z^3\mathbb{1}\,|LC_4\rangle=+\,|LC_4\rangle\,, \tag{110a}$$
$$\sigma_x^1\sigma_y^2\sigma_y^3\sigma_x^4\,|LC_4\rangle=+\,|LC_4\rangle\,, \tag{110b}$$
$$\sigma_y^1\sigma_y^2\sigma_z^3\mathbb{1}\,|LC_4\rangle=-\,|LC_4\rangle\,, \tag{110c}$$
$$\sigma_y^1\sigma_x^2\sigma_y^3\sigma_x^4\,|LC_4\rangle=+\,|LC_4\rangle\,. \tag{110d}$$

In the LHV models, σ_i are assumed to have definite values $v_i=\pm1$, it follows that

$$v_x^1v_x^2v_z^3=+1, \tag{111a}$$
$$v_x^1v_y^2v_y^3v_x^4=+1, \tag{111b}$$
$$v_y^1v_y^2v_z^3=-1, \tag{111c}$$
$$v_y^1v_x^2v_y^3v_x^4=+1. \tag{111d}$$

When one multiplies the above four equations, the left-hand side gives $(v_x^1)^2(v_y^1)^2(v_x^2)^2(v_y^2)^2(v_y^3)^2(v_z^3)^2(v_x^4)^2=+1$, but the right-hand side gives the quantum prediction as -1, thus leads to the sharp contradiction of "$+1_{\rm C}=-1_{\rm Q}$".

Example 8.—For the graph as Fig. 1(h), $m=4, n=3$. The ground state is $|G\rangle=(1/4)(1,1,1,-1,1,-1,1,1,1,1,-1,1,-1,1,1,1)^T$. We consider the vertex 1 and its link vertices $2,3$. From Theorem 1, we have $\{a_2=1, a_3=1\}$, the GHZ-type paradox can be arisen from the following 4 operators:

$$S_1=\sigma_x^1\sigma_z^2\sigma_z^3\mathbb{1}, \tag{112a}$$
$$-S_1S_2S_3=\sigma_x^1\sigma_y^2\sigma_y^3\mathbb{1}, \tag{112b}$$
$$S_1S_2=\sigma_y^1\sigma_y^2\sigma_z^3\sigma_z^4, \tag{112c}$$
$$S_1S_3=\sigma_y^1\sigma_z^2\sigma_y^3\sigma_z^4, \tag{112d}$$

i.e., $S_1|G\rangle=+|G\rangle$, $-S_1S_2S_3|G\rangle=-|G\rangle$, $S_1S_2|G\rangle=+|G\rangle$, $S_1S_3|G\rangle=+|G\rangle$.

Through the unitary transformation $\mathcal{U}=U_1\otimes U_1\otimes U_1\otimes U_1$, with $U_1=(\sigma_x+\sigma_z)/\sqrt{2}$, then the state $|G\rangle$ is equivalent to the cluster state $|CL_4\rangle=(|0000\rangle+|0110\rangle+|1001\rangle-|1111\rangle)/2$, and the 4 operators become

$$E_1=\sigma_z^1\sigma_x^2\sigma_x^3\mathbb{1}, \tag{113a}$$
$$E_2=\sigma_z^1\sigma_y^2\sigma_y^3\mathbb{1}, \tag{113b}$$
$$E_3=\sigma_y^1\sigma_y^2\sigma_x^3\sigma_x^4, \tag{113c}$$
$$E_4=\sigma_y^1\sigma_x^2\sigma_y^3\sigma_x^4, \tag{113d}$$

It can be constructed the 4-qubit GHZ paradox:

$$\sigma_z^1\sigma_x^2\sigma_x^3\mathbb{1}\,|CL_4\rangle=+\,|CL_4\rangle\,, \tag{114a}$$
$$\sigma_z^1\sigma_y^2\sigma_y^3\mathbb{1}\,|CL_4\rangle=-\,|CL_4\rangle\,, \tag{114b}$$
$$\sigma_y^1\sigma_y^2\sigma_x^3\sigma_x^4\,|CL_4\rangle=+\,|CL_4\rangle\,, \tag{114c}$$
$$\sigma_y^1\sigma_x^2\sigma_y^3\sigma_x^4\,|CL_4\rangle=+\,|CL_4\rangle\,. \tag{114d}$$

In LHV models, σ_i are assumed to have definite values $v_i = \pm 1$, it follows that

$$v_z^1 v_x^2 v_x^3 = +1, \tag{115a}$$
$$v_z^1 v_y^2 v_y^3 = -1, \tag{115b}$$
$$v_y^1 v_y^2 v_x^3 v_x^4 = +1, \tag{115c}$$
$$v_y^1 v_x^2 v_y^3 v_x^4 = +1. \tag{115d}$$

When one multiplies the above four equations, the left-hand side gives $(v_y^1)^2(v_z^1)^2(v_x^2)^2(v_y^2)^2(v_x^3)^2(v_y^3)^2(v_x^4)^2 = +1$, but the right-hand side gives the quantum prediction as -1, thus leads to the sharp contradiction of "$+1_{\rm C} = -1_{\rm Q}$".

Example 9.—For the graph as Fig. 1(i), $m = 4, n = 3$. The ground state is $|G\rangle = (1/4)(1,1,1,-1,1,-1,-1,-1,1,1,-1,1,-1,1,-1,-1)^T$. We consider the vertex 1 and its link vertices $2, 3$. From Theorem 1, we have $\{a_1 = 1, a_3 = 2\}$, the GHZ-type paradox can be arisen from the following 4 operators:

$$S_1 = \sigma_x^1 \sigma_z^2 \sigma_z^3 \mathbb{1}, \tag{116a}$$
$$-S_1 S_2 S_3 = \sigma_x^1 \sigma_x^2 \sigma_x^3 \mathbb{1}, \tag{116b}$$
$$S_2 = \sigma_z^1 \sigma_x^2 \sigma_z^3 \sigma_z^4, \tag{116c}$$
$$S_3 = \sigma_z^1 \sigma_z^2 \sigma_x^3 \sigma_z^4, \tag{116d}$$

i.e., $S_1|G\rangle = +|G\rangle$, $-S_1S_2S_3|G\rangle = -|G\rangle$, $S_2|G\rangle = +|G\rangle$, $S_3|G\rangle = +|G\rangle$.

Through the unitary transformation $\mathcal{U} = U_1 \otimes U_2 \otimes U_2 \otimes U_3$, with $U_1 = (\mathbb{1} - i\sigma_x + i\sigma_y - i\sigma_z)/2, U_2 = (\mathbb{1} + i\sigma_x + i\sigma_y - i\sigma_z)/2, U_3 = (\sigma_x + \sigma_z)/\sqrt{2}$, the state $|G\rangle$ is equivalent to the state $|CL_4\rangle = (|0000\rangle + |0110\rangle + |1001\rangle - |1111\rangle)/2$, and the 4 operators become

$$E_1 = \sigma_z^1 \sigma_x^2 \sigma_x^3 \mathbb{1}, \tag{117a}$$
$$E_2 = \sigma_z^1 \sigma_y^2 \sigma_y^3 \mathbb{1}, \tag{117b}$$
$$E_3 = \sigma_y^1 \sigma_y^2 \sigma_x^3 \sigma_x^4, \tag{117c}$$
$$E_4 = \sigma_y^1 \sigma_x^2 \sigma_y^3 \sigma_x^4. \tag{117d}$$

It can be constructed the 4-qubit GHZ paradox:

$$\sigma_z^1 \sigma_x^2 \sigma_x^3 \mathbb{1} |CL_4\rangle = +|CL_4\rangle, \tag{118a}$$
$$\sigma_z^1 \sigma_y^2 \sigma_y^3 \mathbb{1} |CL_4\rangle = -|CL_4\rangle, \tag{118b}$$
$$\sigma_y^1 \sigma_y^2 \sigma_x^3 \sigma_x^4 |CL_4\rangle = +|CL_4\rangle, \tag{118c}$$
$$\sigma_y^1 \sigma_x^2 \sigma_y^3 \sigma_x^4 |CL_4\rangle = +|CL_4\rangle. \tag{118d}$$

In LHV models, σ_i are assumed to have definite values $v_i = \pm 1$, it follows that

$$v_z^1 v_z^2 v_x^3 = +1, \tag{119a}$$
$$v_z^1 v_y^2 v_y^3 = -1, \tag{119b}$$
$$v_y^1 v_y^2 v_x^3 v_x^4 = +1, \tag{119c}$$
$$v_y^1 v_z^2 v_y^3 v_x^4 = +1. \tag{119d}$$

When one multiplies the above four equations, the left-hand side gives $(v_y^1)^2(v_z^1)^2(v_y^2)^2(v_z^2)^2(v_x^3)^2(v_y^3)^2(v_x^4)^2 = +1$, but the right-hand side gives the quantum prediction as -1, thus leads to the sharp contradiction of "$+1_{\rm C} = -1_{\rm Q}$".

Remark 4.—From the above 9 examples for the 3-qubit and 4-qubit systems,, one can observe that (i) the ground state $|G\rangle$ of the Hamiltonian $\mathcal{H}$ is unique, and (ii) the ground state is either the GHZ state or the cluster state. The similar results can be directly generalized to an arbitrary m-qubit system, thus one can obtain the GHZ-type paradox for either the m-qubit GHZ state $|G_m\rangle$ or the m-qubit cluster state $|C_m\rangle$, see Fig. (2).

C. Scope of unique state verification

From the form of Theorem 1, when n is odd, any $n-1$ operator Es can still generate the $n-1$ qubits stabilizing group, so their grand total cannot have degenerate ground state. Furthermore, in the case of $n = m$, there is no unmeasured qubits and the GHZ-type paradox constructed from operator Es can uniquely pick out $|G\rangle$.

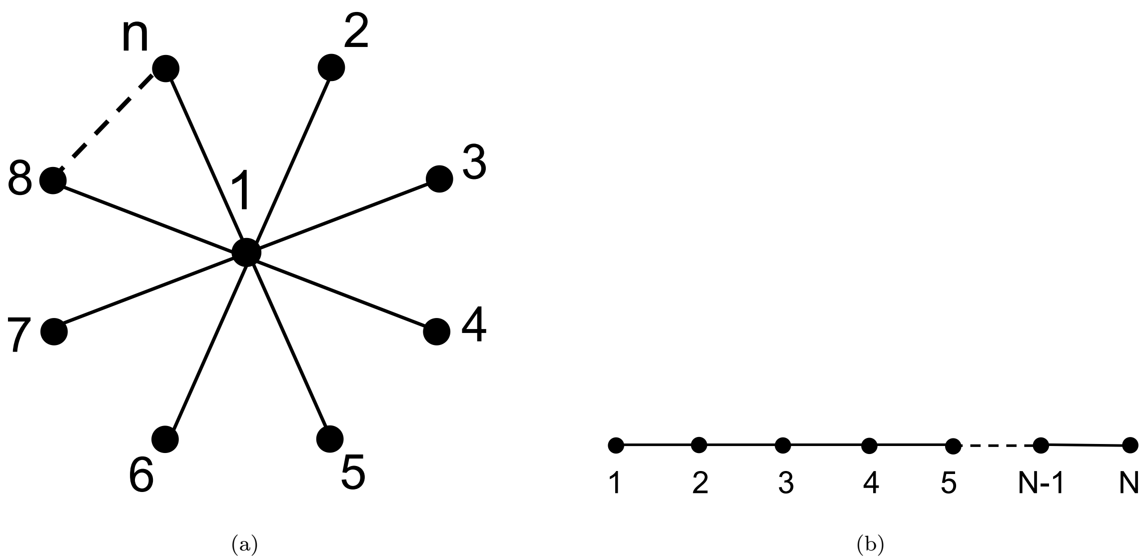

Supplementary Figure 2. Two graphs for the m-qubit system. (a) The graph is the generalization of Fig. 1(a). The corresponding ground state of the Hamiltonian $\mathcal{H}$ is the m-qubit GHZ state $|G_m\rangle = \frac{1}{\sqrt{2}}(|00\cdots 0\rangle + |11\cdots 1\rangle)$ under a local unitary transformation, and the scenario of the GHZ-type paradox is $(m, n) = (m, m)$. (b) The graph is the generalization of Fig. 1(g). The ground state of the Hamiltonian $\mathcal{H}$ is the m-qubit cluster state $|C_m\rangle$, and the scenario of the GHZ-type paradox is $(m, n) = (m, 3)$.

At first glance, the requirement of $n = m$ seems to fail for most of graph states. However, by applying local complementation, a lot of graph states can be reciprocally transformed, and a surprisingly high proportion of graph states have equivalent representations which have universal vertices. The complete orbits of a graph state under possible local complementations can be obtained with computer programming [7]. Shown in Fig. 3b, for $m \leq 9$, one finds that 519 out of 591 possible graph states can be locally complemented to obtain a universal vertex. For the case of $m = 9$, 392 different graph states have their unique GHZ-type paradox that can be in turn exploited to verify the graph states.

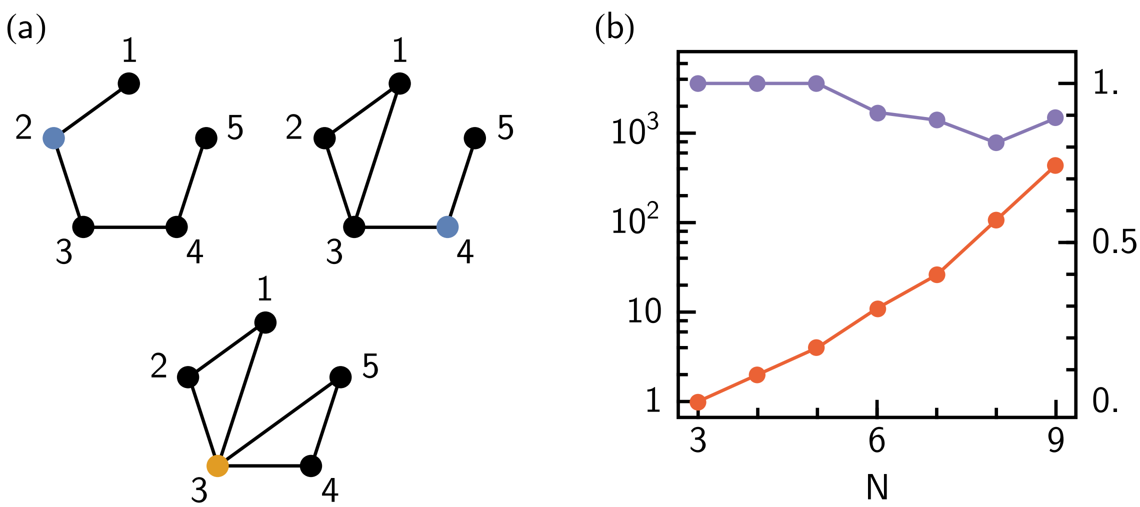

Supplementary Figure 3. The application of local complementation together with Theorem 1. (a) consecutively applying local complementation on the blue vertex of the graph corresponding to $|G_5\rangle$ results in a universal vertex (orange). (b) The total number (purple) of different graph states up to permutation of vertices and local complementation, and the percentage (red) of graph states in which a universal vertex can arise upon applying local complementations.

Example.— The mathematical tool of local complementation [8] together with the theorem 1 can be utilized to construct a genuine multipartite GHZ-type paradox for the 5-qubit linear cluster state $|LC_5\rangle = \bigotimes_{i=1}^{5}(|0\rangle + |1\rangle\, \sigma_z^{i+1})/4\sqrt{2}$. Here, the phrase "genuine" means that the paradox cannot be re-produced by any biseparable quantum system. A local complementation on vertices i transforms the graph state according to $|G\rangle \to e^{-i\pi\sigma_x^i/4}e^{-i\pi\sigma_z^j/4}\,|G\rangle$, where j denotes any vertices in the neighborhood of i, i.e., $C_i^j = 1$. $|LC_5\rangle$ is associated with the graph of five vertices, consecutively connected by four edges, and stabilized by $\{S_1 = \sigma_x^1\sigma_z^2\mathbb{1}^3\mathbb{1}^4\mathbb{1}^5,\ S_2 = \sigma_z^1\sigma_x^2\sigma_z^3\mathbb{1}^4\mathbb{1}^5,\ S_3 = \mathbb{1}^1\sigma_z^2\sigma_x^3\sigma_z^4\mathbb{1}^5,$ $S_4 = \mathbb{1}^1\mathbb{1}^2\sigma_z^3\sigma_x^4\sigma_z^5$, and $S_5 = \mathbb{1}^1\mathbb{1}^2\mathbb{1}^3\sigma_z^4\sigma_x^5,\}$. The graph does not have any universal vertices. However, as shown in Fig.3a, by applying local complementation at vertices 2 and 4, the vertex 3 becomes universal and can be exploited to construct a GHZ-type paradox, in which two-settings applies to every qubit. By reverting the local complementations, the operators are shown to be $E_1 = -S_2S_3S_4$, $E_2 = S_3S_4, E_3 = S_2S_3, E_4 = S_1, E_5 = S_5$, and $E_6 = S_1S_3S_5$, and the following equations hold:

$$[E_1 = \sigma_z^1\sigma_y^2\sigma_x^3\sigma_y^4\sigma_z^5]\ \ |LC_5\rangle = -\,|LC_5\rangle\,, \tag{120a}$$
$$[E_2 = \mathbb{1}^1\sigma_z^2\sigma_y^3\sigma_y^4\sigma_z^5]\ \ |LC_5\rangle = +\,|LC_5\rangle\,, \tag{120b}$$
$$[E_3 = \sigma_z^1\sigma_y^2\sigma_y^3\sigma_z^4\mathbb{1}^5]\ \ |LC_5\rangle = +\,|LC_5\rangle\,, \tag{120c}$$
$$[E_4 = \sigma_x^1\sigma_z^2\mathbb{1}^3\mathbb{1}^4\mathbb{1}^5]\ \ |LC_5\rangle = +\,|LC_5\rangle\,, \tag{120d}$$
$$[E_5 = \mathbb{1}^1\mathbb{1}^2\mathbb{1}^3\sigma_z^4\sigma_x^5]\ \ |LC_5\rangle = +\,|LC_5\rangle\,, \tag{120e}$$
$$[E_6 = \sigma_x^1\mathbb{1}^2\sigma_x^3\mathbb{1}^4\sigma_x^5]\ \ |LC_5\rangle = +\,|LC_5\rangle\,. \tag{120f}$$

From (120), one has $\langle E_i\rangle_{\rm QM} = {\rm Tr}[|LC_5\rangle\langle LC_5|\,E_i] = -1$. Here, $\langle\cdot\rangle_{QM}$ denotes the prediction of an observable given by quantum theory. However, a LHV model assumes the observable σ_i's to have definite values $v_i = \pm 1$ even before the measurements, so it requires $-v_z^1v_y^2v_x^3v_y^4v_z^5 = -1, v_z^2v_y^3v_y^4v_z^5 = +1, v_z^1v_y^2v_y^3v_z^4 = +1, v_x^1v_z^2 = +1, v_z^4v_x^5 = +1$ and $v_x^1v_x^3v_x^5 = +1$. Consequently, when one multiplies the above six equations, the left-hand side gives $-(v_x^1)^2(v_x^3)^2(v_x^5)^2(v_y^2)^2(v_y^3)^2(v_y^4)^2(v_z^1)^2(v_z^2)^2(v_z^4)^2(v_z^5)^2 = +1$, but the right-hand side gives $\prod_{i=1}^{6}\langle E_i\rangle = -1$, thus leading to the sharp contradiction of "$+1_{\rm C} = -1_{\rm Q}$". To confirm the GHZ-type paradox is genuine, one can directly solve the eigensystem of $\mathcal{H}'$ to show the ground state of $\mathcal{H}' = -\sum_{i=1}^{6}E_i$ is non-degenerate, so this GHZ-type paradox is strictly limited to the quinquepartite entangled system of $|LC_5\rangle$.

D. Entanglement detection

Bell's inequality constructed by GHZ-type paradox as

$$\mathcal{I}_n = \sum_{i=1}^{n+1} f_i\,\langle E_i\rangle \overset{\rm LHV}{\leq} n-1, \tag{121}$$

with $f_i = \langle G|E_i|G\rangle \in \{+1,-1\}$, and the maximal violation is directly given by $\mathcal{I}_n^{\rm QM} = n+1$.

The eigenvalues and eigenstates of Bell operator $\sum_{i=1}^{n+1} f_iE_i$ is list in Table. 6, so,

$$\sum_{i=1}^{n+1} f_iE_i = (n+1)\,|G\rangle\langle G| + (n-3)\sum_{k=1}^{\chi_1}|\psi_{n-3}^k\rangle\langle\psi_{n-3}^k| + \cdots + (-n-1)\sum_{k=1}^{\chi_{\frac{n+1}{2}}}|\psi_{-n-1}^k\rangle\langle\psi_{-n-1}^k|\,. \tag{122}$$

For any given state $|\psi\rangle$

$$|\psi\rangle = a\,|G\rangle + \sqrt{1-a^2}\,|G^\perp\rangle\,, \tag{123}$$

Supplementary Table 6. The eigenvalues and eigenstates of Bell operator $\sum_{i=1}^{n+1} f_iE_i$, where the degeneracy satisfy $1+\sum_{j=1}^{\frac{n+1}{2}}\chi_j = 2^n$.

Eigenvalues	$n+1$	$n-3$	$n-7$	$\cdots$	$-n-1$
Degeneracy	1	χ_1	χ_2	$\cdots$	$\chi_{\frac{n+1}{2}}$
Eigenstates	$\|G\rangle$	$\|\psi_{n-3}^1\rangle, \|\psi_{n-3}^2\rangle, \cdots, \|\psi_{n-3}^{\chi_1}\rangle$	$\|\psi_{n-7}^1\rangle, \|\psi_{n-7}^2\rangle, \cdots, \|\psi_{n-7}^{\chi_2}\rangle$	$\cdots$	$\|\psi_{-n-1}^1\rangle, \|\psi_{-n-1}^2\rangle, \cdots, \|\psi_{-n-1}^{\chi_{\frac{n+1}{2}}}\rangle$

where the coefficients $\langle G\,|G^{\perp}\rangle = 0$, $|G^{\perp}\rangle = \sum_{j=1}^{\frac{n+1}{2}} \sum_{k=1}^{\chi_j} b_j^k \,|\psi_{n+1-4j}^k\rangle$, and $\sum_{j=1}^{\frac{n+1}{2}} \sum_{k=1}^{\chi_j} |b_j^k|^2 = 1$.

The fidelity of $|\psi\rangle$ is defined as

$$F = |\,\langle G|\,\psi\rangle|^2 = |a|^2. \tag{124}$$

The violation value of the Bell operator for $|\psi\rangle$ is

$$\begin{aligned}\mathcal{I}_n &= |a|^2 \langle G| \sum_{i=1}^{n+1} f_i E_i \,|G\rangle + (1-|a|^2) \langle G^{\perp}| \sum_{i=1}^{n+1} f_i E_i \,|G^{\perp}\rangle \\ &= |a|^2 (n+1) + (1-|a|^2) \sum_{j=1}^{\frac{n+1}{2}} \sum_{k=1}^{\chi_j} (n+1-4j)|b_j^k|^2. \end{aligned} \tag{125}$$

Due to $0 \leq |b_j^k| \leq 1$, then

$$|a|^2(n+1) + (1-|a|^2)(-n-1) \leq \mathcal{I}_n \leq |a|^2(n+1) + (1-|a|^2)(n-3), \tag{126}$$

so, we can get

$$\frac{\mathcal{I}_n - n + 3}{4} \leq |a|^2 \leq \frac{\mathcal{I}_n + n + 1}{2n+2}, \tag{127}$$

Therefore, the fidelity F of $|\psi\rangle$ is sandwiched between $(\mathcal{I}_n - n + 3)/4$ and $(\mathcal{I}_n + n + 1)/(2n+2)$.

When $|\psi\rangle$ violate the inequality (121), i.e., $\mathcal{I}_n > n-1$, then $F = |a|^2 \geq (\mathcal{I}_n - n + 3)/4 > 1/2$. Therefore, the violation of (121) guarantees at least 50% fidelity to the target state $|G\rangle$. Vice versa, for any given state $|\psi\rangle$, it is possible to violate the inequality (121) only when its fidelity to the target graph state $|G\rangle$ is greater than 50%. And the fidelity of all biseparable states are less than 50%. Remarkably, this is also effective for mixed states ρ, that only if the proportion of $\rho_G = |G\rangle\langle G|$ greater than 50%, it is possible to violate the inequality (121).

Proof:

The fidelity of ρ with respect to the target graph state $|G\rangle$ is

$$F = \langle G|\,\rho\,|G\rangle = |a|^2, \tag{128}$$

and

$$Tr[|\psi_j^k\rangle\langle\psi_j^k|\,\rho] = \langle\psi_j^k|\,\rho\,|\psi_j^k\rangle = (1-|a|^2)|c_j^k|^2, \tag{129}$$

where $\sum_{j=1}^{\frac{n+1}{2}} \sum_{k=1}^{\chi_j} |c_j^k|^2 = 1$.

Then, the violation value of the Bell operator for ρ is

$$\begin{aligned}\mathcal{I}_n &= Tr((\sum_{i=1}^{n+1} f_i E_i)\cdot\rho) \\ &= (n+1)\langle G|\,\rho\,|G\rangle + (n-3)\sum_{k=1}^{\chi_1} \langle\psi_{n-3}^k|\,\rho\,|\psi_{n-3}^k\rangle + \cdots + (-n-1)\sum_{k=1}^{\chi_{\frac{n+1}{2}}} \langle\psi_{-n-1}^k|\,\rho\,|\psi_{-n-1}^k\rangle \\ &= |a|^2(n+1) + (1-|a|^2)(n-3)\sum_{k=1}^{\chi_1} |c_{n-3}^k|^2 + \cdots + (1-|a|^2)(-n-1)\sum_{k=1}^{\chi_{\frac{n+1}{2}}} |c_{-n-1}^k|^2 \\ &= |a|^2(n+1) + (1-|a|^2)\sum_{j=1}^{\frac{n+1}{2}} \sum_{k=1}^{\chi_j} (n+1-4j)|c_j^k|^2. \end{aligned} \tag{130}$$

Similarly as the calculations of Eq. (125)-(127), we can get the fidelity $(\mathcal{I}_n - n + 3)/4 \leq F = |a|^2 \leq (\mathcal{I}_n + n + 1)/(2n+2)$. Therefore, the fidelity greater than 50% if the the inequality (121) is violated.

E. New quantum states that can possess the GHZ-type paradox

The significance of Theorem 1 is two-folded: (i) It has provided a unified approach to reveal the GHZ-type paradoxes for two important quantum states (i.e., the m-qubit GHZ state and the m-qubit cluster state), which naturally recovers the previous result in the literature. (ii) It has provided an interesting guidance or clue, i.e., quantum states that can possess the GHZ-type paradox are usually the ground states of some specific Hamiltonians.

Besides the GHZ state and the cluster state, there are indeed other new quantum states that can also possess the GHZ-type paradox, and importantly they can be similarly generated from the ground states of some Hamiltonians. In the following, we would like to give two examples.

Example 10.— In *Example 7*, for the 4-qubit cluster state $|LC_4\rangle$, we have already derived the following 4 operators (see Eq. (109a)):

$$\begin{aligned} E_1 &= \sigma_x^1\sigma_x^2\sigma_z^3\mathbb{1}, &(131a)\\ E_2 &= \sigma_x^1\sigma_y^2\sigma_y^3\sigma_x^4, &(131b)\\ E_3 &= \sigma_y^1\sigma_y^2\sigma_z^3\mathbb{1}, &(131c)\\ E_4 &= \sigma_y^1\sigma_x^2\sigma_y^3\sigma_x^4. &(131d)\end{aligned}$$

which satisfy (see Eq. (110))

$$\begin{aligned} [E_1 &= \sigma_x^1\sigma_x^2\sigma_z^3\mathbb{1}]\,|LC_4\rangle = +\,|LC_4\rangle\,, &(132a)\\ [E_2 &= \sigma_x^1\sigma_y^2\sigma_y^3\sigma_x^4]\,|LC_4\rangle = +\,|LC_4\rangle\,, &(132b)\\ [E_3 &= \sigma_y^1\sigma_y^2\sigma_z^3\mathbb{1}]\,|LC_4\rangle = -\,|LC_4\rangle\,, &(132c)\\ [E_4 &= \sigma_y^1\sigma_x^2\sigma_y^3\sigma_x^4]\,|LC_4\rangle = +\,|LC_4\rangle\,. &(132d)\end{aligned}$$

Based on the operators E_i's, let us define the following Hamiltonian

$$\mathcal{H}' = -(E_1 + E_2 + E_4) + E_3, \tag{133}$$

whose ground states are interestingly two-folded degeneracies, i.e.,

$$\mathcal{H}'\,|LC_4\rangle = -4\,|LC_4\rangle\,, \qquad \mathcal{H}'\,|LC_4'\rangle = -4\,|LC_4'\rangle\,, \tag{134}$$

with

$$\begin{aligned} |LC_4\rangle &= \frac{1}{2}(|0000\rangle + |0011\rangle + |1100\rangle - |1111\rangle),\\ |LC_4'\rangle &= \frac{1}{2}(|0001\rangle + |0010\rangle + |1101\rangle - |1110\rangle),\\ &= (\mathbb{1}\otimes\mathbb{1}\otimes\mathbb{1}\otimes\sigma_x)\,|LC_4\rangle\,. &(135a)\end{aligned}$$

Let us define the following 4-qubit extended cluster state:

$$\begin{aligned} |LC_4(\theta)\rangle &= \cos\theta\,|LC_4\rangle + \sin\theta\,|LC_4'\rangle\\ &= \cos\theta(|0000\rangle + |0011\rangle + |1100\rangle - |1111\rangle)/2 + \sin\theta(|0001\rangle + |0010\rangle + |1101\rangle - |1110\rangle)/2, &(136)\end{aligned}$$

Similar to Eq. (132), for the new quantum state $|LC_4(\theta)\rangle$, one has the following GHZ-type paradox

$$\begin{aligned} [E_1 &= \sigma_x^1\sigma_x^2\sigma_z^3\mathbb{1}]\,|LC_4(\theta)\rangle = +\,|LC_4(\theta)\rangle\,, &(137a)\\ [E_2 &= \sigma_x^1\sigma_y^2\sigma_y^3\sigma_x^4]\,|LC_4(\theta)\rangle = +\,|LC_4(\theta)\rangle\,, &(137b)\\ [E_3 &= \sigma_y^1\sigma_y^2\sigma_z^3\mathbb{1}]\,|LC_4(\theta)\rangle = -\,|LC_4(\theta)\rangle\,, &(137c)\\ [E_4 &= \sigma_y^1\sigma_x^2\sigma_y^3\sigma_x^4]\,|LC_4(\theta)\rangle = +\,|LC_4(\theta)\rangle\,, &(137d)\end{aligned}$$

that is valid for arbitrary parameter θ. It is easy to have the quantum prediction as

$$\mathcal{Q} = \prod_{i=1}^{4}\langle LC_4(\theta)|E_i|LC_4(\theta)\rangle = -1. \tag{138}$$

Remark. 5—Thus we have derived a new family of pure states $|LC_4(\theta)\rangle$, which can also possess the GHZ-type paradox. The difference is that the usual cluster state $|LC_4\rangle = |LC_4(\theta = 0)\rangle$ is a graph state, while the state $|LC_4(\theta)\rangle$ is generally not a graph state, because it is not the common eigenstate of operators $\{S_1, S_2, S_3, S_4\}$.

Remark. 6—When $\theta = \pi/4$, we have

$$\begin{aligned} |LC_4(\theta = \pi/4)\rangle &= \frac{1}{2}(|0000\rangle + |0011\rangle + |1100\rangle - |1111\rangle) + \frac{1}{2}(|0001\rangle + |0010\rangle + |1101\rangle - |1110\rangle) \\ &= \frac{1}{\sqrt{2}}(|000\rangle + |001\rangle + |110\rangle - |111\rangle) \otimes \frac{1}{\sqrt{2}}(|0\rangle + |1\rangle) \\ &= \frac{1}{\sqrt{2}}(|00+\rangle + |11-\rangle) \otimes |+\rangle \,. \end{aligned} \tag{139}$$

Through the local unitary transformation (LUT) $\mathcal{U} = \mathbb{1} \otimes \mathbb{1} \otimes U_1 \otimes \mathbb{1}$, with $U_1 = (\sigma_x + \sigma_z)/\sqrt{2}$, $|LC_4(\theta = \pi/4)\rangle$ is equivalent to a *bi-separable state*:

$$|LC_4(\theta = \pi/4)\rangle \overset{\text{LUT}}{=} |GHZ_3\rangle \otimes |+\rangle = (|000\rangle + |111\rangle) \otimes |+\rangle \,. \tag{140}$$

Remark 7.—Let us consider the following mixed state

$$\rho(\theta) = \cos^2\theta |LC_4\rangle\langle LC_4| + \sin^2\theta |LC_4'\rangle\langle LC_4'|, \tag{141}$$

which is a convex sum of two cluster states. It can be verified that the quantum prediction is

$$\begin{aligned} \mathcal{Q} &= \prod_{i=1}^{4} \mathrm{tr}[\rho(\theta) E_i] \\ &= \cos^2\theta \prod_{i=1}^{4} \langle LC_4|E_i|LC_4\rangle + \sin^2\theta \prod_{i=1}^{4} \langle LC_4'|E_i|LC_4'\rangle \\ &= -\cos^2\theta - \sin^2\theta \\ &= -1, \end{aligned} \tag{142}$$

which is θ-independent. Thus, for the first time, we have encountered that a mixed state (such as $\rho(\theta)$ in Eq. (141)) can also possess the GHZ-type paradox.

Example 12.—In *Example 3*, for the 4-qubit GHZ state, we have obtained the following operators (see Eq. (93a)):

$$E_1 = \sigma_x^1 \sigma_x^2 \sigma_x^3 \sigma_x^4, \tag{143a}$$
$$E_2 = \sigma_x^1 \sigma_y^2 \sigma_y^3 \sigma_x^4, \tag{143b}$$
$$E_3 = \sigma_x^1 \sigma_x^2 \sigma_y^3 \sigma_y^4, \tag{143c}$$
$$E_4 = \sigma_x^1 \sigma_y^2 \sigma_x^3 \sigma_y^4. \tag{143d}$$

Similarly, we define the new Hamiltonian as $\mathcal{H}' = -E_1 + (E_2 + E_3 + E_4)$, then we can get two ground states, which are two-fold degeneracy:

$$|GHZ_4\rangle = \frac{1}{\sqrt{2}}(|0000\rangle + |1111\rangle), \tag{144a}$$

$$\begin{aligned} |GHZ_4'\rangle &= \frac{1}{\sqrt{2}}(|0111\rangle + |1000\rangle) \\ &= (\sigma_x \otimes \mathbb{1} \otimes \mathbb{1} \otimes \mathbb{1})|GHZ_4\rangle, \end{aligned} \tag{144b}$$

with $\mathcal{H}'|GHZ_4\rangle = -4|GHZ_4\rangle$ and $\mathcal{H}'|GHZ_4'\rangle = -4|GHZ_4'\rangle$.

Let us define the following 4-qubit extended GHZ state

$$\begin{aligned} |GHZ_4(\theta)\rangle &= \cos\theta |GHZ_4\rangle + \sin\theta |GHZ_4'\rangle \\ &= \cos\theta(|0000\rangle + |1111\rangle)/\sqrt{2} + \sin\theta(|0111\rangle + |1000\rangle)/\sqrt{2}, \end{aligned} \tag{145}$$

which is the superposition state of two 4-qubit GHZ state. For the new quantum state $GHZ_4(\theta)$, one has the following GHZ-type paradox

$$[E_1 = \sigma_x^1 \sigma_x^2 \sigma_x^3 \sigma_x^4]|GHZ_4(\theta)\rangle = +|GHZ_4(\theta)\rangle, \tag{146a}$$
$$[E_2 = \sigma_x^1 \sigma_y^2 \sigma_y^3 \sigma_x^4]|GHZ_4(\theta)\rangle = -|GHZ_4(\theta)\rangle, \tag{146b}$$
$$[E_3 = \sigma_x^1 \sigma_x^2 \sigma_y^3 \sigma_y^4]|GHZ_4(\theta)\rangle = -|GHZ_4(\theta)\rangle, \tag{146c}$$
$$[E_4 = \sigma_x^1 \sigma_y^2 \sigma_x^3 \sigma_y^4]|GHZ_4(\theta)\rangle = -|GHZ_4(\theta)\rangle, \tag{146d}$$

that is valid for arbitrary parameter θ.

Remark. 8—Thus we have derived aother new family of pure states $|GHZ_4(\theta)\rangle$, which can also possess the GHZ-type paradox. The difference is that the usual GHZ state $|GHZ_4\rangle = |LC_4(\theta=0)\rangle$ is a graph state, while the state $|GHZ_4(\theta)\rangle$ is generally not, because it is not the common eigenstate of operators $\{S_1, S_2, S_3, S_4\}$. When $\theta = \pi/4$, we have

$$\begin{aligned} |GHZ_4(\theta=\pi/4)\rangle &= \frac{1}{2}(|0000\rangle + |1111\rangle) + \frac{1}{2}(|0111\rangle + |1000\rangle) \\ &= \frac{1}{\sqrt{2}}(|0\rangle + |1\rangle) \otimes \frac{1}{\sqrt{2}}(|000\rangle + |111\rangle) \\ &= |+\rangle\, |GHZ_3\rangle\,, \end{aligned} \tag{147}$$

which is equivalent to $|LC_4(\theta=\pi/4)\rangle$ after permuting some qubits.

Remark 9.—Let us consider the following mixed state

$$\rho(\theta) = \cos^2\theta |GHZ_4\rangle\langle GHZ_4| + \sin^2\theta |GHZ'_4\rangle\langle GHZ'_4|. \tag{148}$$

Similar to *Example 10*, such a mixed state can also possess the GHZ-type paradox.

F. Converting the GHZ-type paradox into the perfect Hardy-type paradox

The GHZ proof is only valid for the quantum system with three or more particles. Motivated by this, in 1993 Hardy presented a kind of all-versus-nothing proofs for two qubits [1]. The Hardy's proof can be expressed as follows [2]. Let us denote by $P(A_i < B_j)$ the joint conditional probability for the event $A_i < B_j$, the Hardy's paradox can then be written as

$$\begin{cases} P_1 = P(A_2 < B_1) = 0, \\ P_2 = P(B_1 < A_1) = 0, \\ P_2 = P(A_1 < B_2) = 0, \\ \hline\hline P_{\rm suc} = P(A_2 < B_2) \overset{\rm QM}{=} \left(5\sqrt{5} - 11\right)/2 \approx 0.09 > 0. \end{cases} \tag{149}$$

Here $P(A_i < B_j) = P(A_i = 0, B_j = 1)$ for the two-qubit case. The last equation in (149) equals to zero in the LHV models, because if $A_2 \geq B_1, B_1 \geq A_1, A_1 \geq B_2$, then one must have $A_2 \geq B_2$. But in the QM, when the first three events are satisfied, we can get a value (usually termed as the maximal success probability of nonlocal events) of approximately 0.09 to make the last event $A_2 < B_2$ happen. Although $P_{\rm suc} \approx 0.09$ is quite small, it essentially distinguishes QM from the LHV models. In the Hardy-test experiment, one will measure the success probability $P_{\rm suc}$ under the three constraints. If $P_{\rm suc} \geq 0$, then the experimental result confirms the quantum prediction.

In tradition, the GHZ paradox and Hardy's paradox are two distinct all-versus-nothing proof for Bell's nonlocality. Very recently, the GHZ paradox and Hardy's paradox have been unified into a single framework, and the GHZ paradox can be viewed as a perfect Hardy's paradox [3], in which the seccess probability $P_{\rm suc}$ equals to 1. The GHZ-type paradox can be converted into a perfect Hardy-type paradox. In the following, we give two examples to illustrate this idea based on Fig. 1(a) and Fig. 1(g).

Example 13.—For the Fig. 1(a), there is a GHZ-type paradox for 3-qubit GHZ state $|GHZ_3\rangle = \frac{1}{\sqrt{2}}(|000\rangle + |111\rangle)$ (this is also the original GHZ paradox [4]):

$$\langle GHZ_3|A_1^1 A_2^2 A_3^2|GHZ_3\rangle = -1, \tag{150a}$$
$$\langle GHZ_3|A_1^2 A_2^1 A_3^2|GHZ_3\rangle = -1, \tag{150b}$$
$$\langle GHZ_3|A_1^2 A_2^2 A_3^1|GHZ_3\rangle = -1, \tag{150c}$$
$$\langle GHZ_3|A_1^1 A_2^1 A_3^1|GHZ_3\rangle = +1, \tag{150d}$$

where $A_1^1 = A_2^1 = A_3^1 = \sigma_x,\; A_1^2 = A_2^2 = A_3^2 = \sigma_y$.

As we have known, the correlation functions can be written in terms of joint probabilities as

$$\begin{aligned}\langle GHZ_3|A_iB_jC_k|GHZ_3\rangle &= \sum_{a,b,c=0}^{1}(-1)^{a+b+c}\,P(A_i=a,B_j=b,C_k=c)\\ &= \sum_{r=0}^{1}(-1)^{r}\,P(A_i+B_j+C_k=r)\end{aligned} \tag{151}$$

with

$$\begin{aligned}P(A_i+B_j+C_k=0) &= P(A_i=0,B_j=0,C_k=0)+P(A_i=1,B_j=1,C_k=0)+\\ &\quad P(A_i=1,B_j=0,C_k=1)+P(A_i=0,B_j=1,C_k=1),\\ P(A_i+B_j+C_k=1) &= P(A_i=1,B_j=0,C_k=0)+P(A_i=0,B_j=1,C_k=0)+\\ &\quad P(A_i=0,B_j=0,C_k=1)+P(A_i=1,B_j=1,C_k=1).\end{aligned} \tag{152}$$

Due to

$$P(A_i+B_j+C_k=0)+P(A_i+B_j+C_k=1)=1, \tag{153}$$

we then have

$$\begin{aligned}\langle GHZ_3|A_iB_jC_k|GHZ_3\rangle &= P(A_i+B_j+C_k=0)-P(A_i+B_j+C_k=1)\\ &= 2P(A_i+B_j+C_k=0)-1\\ &= 1-2P(A_i+B_j+C_k=1).\end{aligned} \tag{154}$$

We can convert the correlation functions of operators into a series of probability form:

$$\langle GHZ_3|A_1^1A_2^2A_3^2|GHZ_3\rangle = -1, \to P(A_1^1+A_2^2+A_3^2=0)=0, \tag{155a}$$
$$\langle GHZ_3|A_1^2A_2^1A_3^2|GHZ_3\rangle = -1, \to P(A_1^2+A_2^1+A_3^2=0)=0, \tag{155b}$$
$$\langle GHZ_3|A_1^2A_2^2A_3^1|GHZ_3\rangle = -1, \to P(A_1^2+A_2^2+A_3^1=0)=0, \tag{155c}$$
$$\langle GHZ_3|A_1^1A_2^1A_3^1|GHZ_3\rangle = +1, \to P(A_1^1+A_2^1+A_3^1=0)\overset{\text{QM}}{=}1>0. \tag{155d}$$

Thus, we have the perfect Hardy-type paradox for the 3-qubit GHZ state as

$$\begin{cases} P(A_1^1+A_2^2+A_3^2=0)=0,\\ P(A_1^2+A_2^1+A_3^2=0)=0,\\ P(A_1^2+A_2^2+A_3^1=0)=0,\\ \hline\hline P(A_1^1+A_2^1+A_3^1=0)\overset{\text{QM}}{=}1>0.\end{cases} \tag{156}$$

Proof. In LHV models, without loss of generality, let us suppose that the output of the observable A_1^1 is 1. Then the first equation in (156) implies $A_2^2+A_3^2=0$. For any output of A_1^2, we have $A_1^2+A_1^2=0$. Thus, the second constraint and the third constraint in (156) lead to $A_2^1+A_3^2+A_2^2+A_3^1=0$, which yields $A_2^1+A_3^1=0$. It thus holds that $A_1^1+A_2^1+A_3^1=1$, i.e., $P(A_1^1+A_2^1+A_3^1=0)=0$.

In QM, for a system in the 3-qubit GHZ state $|GHZ_3\rangle=(|000\rangle+|111\rangle)/\sqrt{2}$ and the measurements chosen as $A_1^1=A_2^1=A_3^1=\sigma_x,\ A_1^2=A_2^2=A_3^2=\sigma_y$, one can see that the first three equations in (156) hold and the success probability $P(A_1^1+A_2^1+A_3^1=0)$ is equal to 1. □

Example 14.—The GHZ-type paradox for 4-qubit GHZ state $|GHZ_4\rangle=\frac{1}{\sqrt{2}}(|0000\rangle+|1111\rangle)$:

$$\langle GHZ_4|A_1^1A_2^2A_3^2A_4^1|GHZ_4\rangle = -1, \tag{157a}$$
$$\langle GHZ_4|A_1^1A_2^1A_3^2A_4^2|GHZ_4\rangle = -1, \tag{157b}$$
$$\langle GHZ_4|A_1^1A_2^2A_3^1A_4^2|GHZ_4\rangle = -1, \tag{157c}$$
$$\langle GHZ_4|A_1^1A_2^1A_3^1A_4^1|GHZ_4\rangle = +1, \tag{157d}$$

where $A_1^1=A_2^1=A_3^1=A_4^1=\sigma_x,\ A_2^2=A_3^2=A_4^2=\sigma_y$.

Similarly, we can convert the correlation functions of operators into a series of probability form:

$$\langle GHZ_4|A_1^1A_2^2A_3^2A_4^1|GHZ_4\rangle = -1, \rightarrow P(A_1^1 + A_2^2 + A_3^2 + A_4^1 = 0) = 0, \tag{158a}$$
$$\langle GHZ_4|A_1^1A_2^1A_3^2A_4^2|GHZ_4\rangle = -1, \rightarrow P(A_1^1 + A_2^1 + A_3^2 + A_4^2 = 0) = 0, \tag{158b}$$
$$\langle GHZ_4|A_1^1A_2^2A_3^1A_4^2|GHZ_4\rangle = -1, \rightarrow P(A_1^1 + A_2^2 + A_3^1 + A_4^2 = 0) = 0, \tag{158c}$$
$$\langle GHZ_4|A_1^1A_2^1A_3^1A_4^1|GHZ_4\rangle = +1, \rightarrow P(A_1^1 + A_2^1 + A_3^1 + A_4^1 = 0) \overset{\text{QM}}{=} 1 > 0. \tag{158d}$$

Thus, we have the perfect Hardy-type paradox for the 3-qubit GHZ state as

$$\begin{cases} P(A_1^1 + A_2^2 + A_3^2 + A_4^1 = 0) = 0, \\ P(A_1^1 + A_2^1 + A_3^2 + A_4^2 = 0) = 0, \\ P(A_1^1 + A_2^2 + A_3^1 + A_4^2 = 0) = 0, \\ \hline\hline P(A_1^1 + A_2^1 + A_3^1 + A_4^1 = 0) \overset{\text{QM}}{=} 1 > 0. \end{cases} \tag{159}$$

Proof. In LHV models, without loss of generality, let us suppose that the output of the observable A_2^2 is 1. Then the first equation in (159) implies $A_1^1 + A_3^2 + A_4^1 = 0$. For any output of A_i^j, we have $A_i^j + A_i^j = 0$. Thus, the second constraint and the third constraint in (159) lead to $A_2^1 + A_3^2 + A_2^2 + A_3^1 = 0$, which yields $A_2^1 + A_3^2 + A_3^1 = 1$. It thus holds that $A_1^1 + A_2^1 + A_3^1 + A_4^1 = 1$, i.e., $P(A_1^1 + A_2^1 + A_3^1 + A_4^1 = 0) = 0$.

In QM, for a system in the 4-qubit GHZ state $|GHZ_4\rangle = (|0000\rangle + |1111\rangle)/\sqrt{2}$ and the measurements chosen as $A_1^1 = A_2^1 = A_3^1 = A_4^1 = \sigma_x$, $A_2^2 = A_3^2 = A_4^2 = \sigma_y$, one can see that the first three equations in (159) hold and the success probability $P(A_1^1 + A_2^1 + A_3^1 + A_4^1 = 0)$ is equal to 1. □

Example 15.—For the Fig. 1(g), there is a GHZ-type paradox for the 4-qubit cluster state $|LC_4\rangle = (|0000\rangle + |0011\rangle + |1100\rangle - |1111\rangle)/2$:

$$\langle LC_4|A_1^1A_2^1A_3^1\mathbb{1}\,|LC_4\rangle = +1, \tag{160a}$$
$$\langle LC_4|A_1^1A_2^2A_3^2A_4^1\,|LC_4\rangle = +1, \tag{160b}$$
$$\langle LC_4|A_1^2A_2^1A_3^2A_4^1\,|LC_4\rangle = +1, \tag{160c}$$
$$\langle LC_4|A_1^2A_2^2A_3^1\mathbb{1}\,|LC_4\rangle = -1, \tag{160d}$$

where $A_1^1 = A_2^1 = A_4^1 = \sigma_x, A_1^2 = A_2^2 = A_3^2 = \sigma_y, A_3^1 = \sigma_z$.

Similarly, we can convert the correlation functions of operators into a series of probability form as

$$\langle LC_4|A_1^1A_2^1A_3^1\mathbb{1}\,|LC_4\rangle = -1, \rightarrow P(A_1^1 + A_2^1 + A_3^1 = 1) = 0, \tag{161a}$$
$$\langle LC_4|A_1^1A_2^2A_3^2A_4^1\,|LC_4\rangle = -1, \rightarrow P(A_1^1 + A_2^2 + A_3^2 + A_4^1 = 1) = 0, \tag{161b}$$
$$\langle LC_4|A_1^2A_2^1A_3^2A_4^1\,|LC_4\rangle = -1, \rightarrow P(A_1^2 + A_2^1 + A_3^2 + A_4^1 = 1), \tag{161c}$$
$$\langle LC_4|A_1^2A_2^2A_3^1\mathbb{1}\,|LC_4\rangle = +1, \rightarrow P(A_1^2 + A_2^2 + A_3^1 = 1) \overset{\text{QM}}{=} 1 > 0. \tag{161d}$$

Thus one obtains the perfect Hardy-type paradox of 4-qubit cluster state as follows

$$\begin{cases} P(A_1^1 + A_2^1 + A_3^1 = 1) = 0, \\ P(A_1^1 + A_2^2 + A_3^2 + A_4^1 = 1) = 0, \\ P(A_1^2 + A_2^1 + A_3^2 + A_4^1 = 1) = 0, \\ \hline\hline P(A_1^2 + A_2^2 + A_3^1 = 1) \overset{\text{QM}}{=} 1 > 0. \end{cases} \tag{162}$$

Proof. In LHV models, without loss of generality, let us suppose that the output of the observable A_1^1 is 1. Then the first equation in (162) implies $A_2^1 + A_3^1 = 1$. For any output of A_2^1, A_3^2 and A_4^1, we have $2A_2^1 = 2A_3^1 = 2A_4^1 = 0$. Thus, the first three equations in (162) lead to $A_1^2 + A_2^2 + A_3^1 = 0$, i.e., $P(A_1^1 + A_2^2 + A_3^2 = 1) = 0$.

In QM, when the system is in the 4-qubit cluster state $|LC_4\rangle = (|0000\rangle + |0011\rangle + |1100\rangle - |1111\rangle)/2$ and the measurements chosen as $A_1^1 = A_2^1 = A_4^1 = \sigma_x, A_1^2 = A_2^2 = A_3^2 = \sigma_y, A_3^1 = \sigma_z$, the successful probability $P(A_1^2 + A_2^2 + A_3^1 = 1) = 1$, which is completely opposite to zero in the LHV models. □

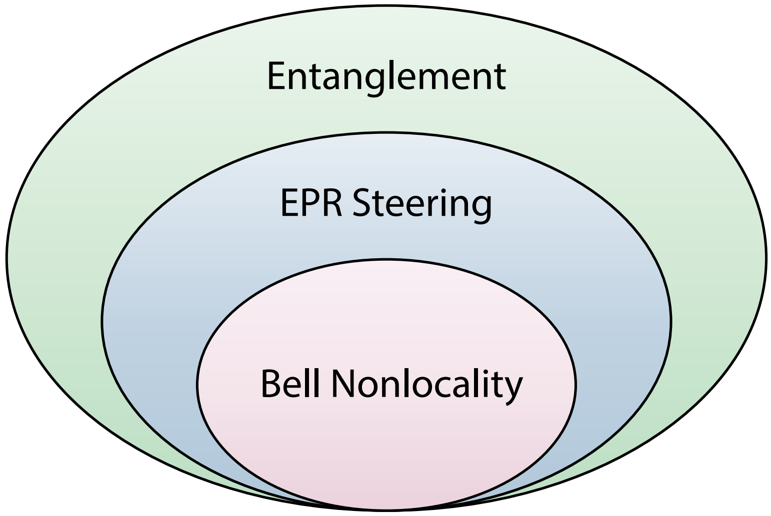

Supplementary Figure 4. Three kinds of quantum nonlocality: quantum entanglement, EPR steering, and Bell's nonlocality

G. EPR steering paradox "$1_{\rm C} = 2_{\rm Q}$"

In Ref. [5], quantum nonlocality has been classified into three different types: quantum entanglement, EPR steering, and Bell's nonlocality. EPR steering is a novel nonlocality that lies between Bell's nonlocality and quantum entanglement (see Fig. 4). Similar to the GHZ paradox "$+1_{\rm C} = -1_{\rm Q}$" in Bell's nonlocality, in the field of EPR steering, there is also an analogue steering paradox "$1_{\rm C} = 2_{\rm Q}$", which was first presented in Ref. [6], but merely limited to the pure states of bipartite system. However, whether the EPR steering paradox is applicable for the mixed state is still an open question. In this section we for the first time show that the mixed state $\rho(\theta)$ in Eq. (141) can possess an analogue GHZ-type paradox, i.e., the EPR steering paradox "$1_{\rm C} = 2_{\rm Q}$".

Let us consider the following mixed state (the same with the one in Eq. (141))

$$\rho(\theta) = \cos^2\theta|LC_4\rangle\langle LC_4| + \sin^2\theta|LC'_4\rangle\langle LC'_4|, \tag{163}$$

with

$$\begin{aligned}|LC_4\rangle &= \frac{1}{2}(|0000\rangle + |0011\rangle + |1100\rangle - |1111\rangle),\\ |LC'_4\rangle &= \frac{1}{2}(|0001\rangle + |0010\rangle + |1101\rangle - |1110\rangle).\end{aligned} \tag{164a}$$

being two orthogonal cluster states. To illustrate the steering paradox "$1_{\rm C} = 2_{\rm Q}$", we need to show the quantum prediction is $\mathcal{Q} = 2$ and the classical prediction (corresponding to the local-hidden-state (LHS) models) is $\mathcal{C} = 1$.

In the steering scenario, Alice prepares the mixed state $\rho(\theta)$ as in Eq. (163). She keeps 3, 4 particles and sends the 1, 2 particles to Bob. To verify the steerability of Alice, Bob asks Alice to perform her choice of either one of two possible projective measurements $\sigma_z\sigma_z$ and $\sigma_y\sigma_x$. In the two-setting steering protocol of $\{\hat{n}_1, \hat{n}_2\}$ ($\hat{n}_1 \neq \hat{n}_2$), with

$$\hat{n}_1 = \sigma_z\sigma_z \equiv zz, \quad \hat{n}_2 = \sigma_y\sigma_x \equiv yx, \tag{165}$$

one has the explicit projectors as

$$\mathcal{P}_{00}^{\hat{n}_1} = |00\rangle\langle 00|, \tag{166a}$$
$$\mathcal{P}_{01}^{\hat{n}_1} = |01\rangle\langle 01|, \tag{166b}$$
$$\mathcal{P}_{10}^{\hat{n}_1} = |10\rangle\langle 10|, \tag{166c}$$
$$\mathcal{P}_{11}^{\hat{n}_1} = |11\rangle\langle 11|, \tag{166d}$$
$$\mathcal{P}_{00}^{\hat{n}_2} = |\uparrow +\rangle\langle\uparrow +|, \tag{166e}$$
$$\mathcal{P}_{01}^{\hat{n}_2} = |\uparrow -\rangle\langle\uparrow -|, \tag{166f}$$
$$\mathcal{P}_{10}^{\hat{n}_2} = |\downarrow +\rangle\langle\downarrow +|, \tag{166g}$$
$$\mathcal{P}_{11}^{\hat{n}_2} = |\downarrow -\rangle\langle\downarrow -|, \tag{166h}$$

where $|\pm\rangle=\frac{1}{\sqrt{2}}(|0\rangle\pm|1\rangle)$ and $|\updownarrow\rangle=\frac{1}{\sqrt{2}}(|0\rangle\pm i|1\rangle)$. Accordingly, Bob's eight unnormalized conditional states are

$$\tilde{\rho}_{00}^{\hat{n}_1}=\mathrm{tr}_{3,4}[(\mathcal{P}_{00}^{\hat{\mathrm{n}}_1}\otimes\mathbb{1})\rho(\theta)]=\frac{1}{4}\cos^2\theta(|00\rangle+|11\rangle)(\langle 00|+\langle 11|), \tag{167a}$$
$$\tilde{\rho}_{01}^{\hat{n}_1}=\mathrm{tr}_{3,4}[(\mathcal{P}_{01}^{\hat{\mathrm{n}}_1}\otimes\mathbb{1})\rho(\theta)]=\frac{1}{4}\sin^2\theta(|00\rangle+|11\rangle)(\langle 00|+\langle 11|), \tag{167b}$$
$$\tilde{\rho}_{10}^{\hat{n}_1}=\mathrm{tr}_{3,4}[(\mathcal{P}_{10}^{\hat{\mathrm{n}}_1}\otimes\mathbb{1})\rho(\theta)]=\frac{1}{4}\sin^2\theta(|00\rangle-|11\rangle)(\langle 00|-\langle 11|), \tag{167c}$$
$$\tilde{\rho}_{11}^{\hat{n}_1}=\mathrm{tr}_{3,4}[(\mathcal{P}_{11}^{\hat{\mathrm{n}}_1}\otimes\mathbb{1})\rho(\theta)]=\frac{1}{4}\cos^2\theta(|00\rangle-|11\rangle)(\langle 00|-\langle 11|), \tag{167d}$$
$$\tilde{\rho}_{00}^{\hat{n}_2}=\mathrm{tr}_{3,4}[(\mathcal{P}_{00}^{\hat{\mathrm{n}}_2}\otimes\mathbb{1})\rho(\theta)]=\frac{1}{8}(|00\rangle+\mathrm{i}|11\rangle)(\langle 00|-\mathrm{i}\langle 11|), \tag{167e}$$
$$\tilde{\rho}_{01}^{\hat{n}_2}=\mathrm{tr}_{3,4}[(\mathcal{P}_{01}^{\hat{\mathrm{n}}_2}\otimes\mathbb{1})\rho(\theta)]=\frac{1}{8}(|00\rangle-\mathrm{i}|11\rangle)(\langle 00|+\mathrm{i}\langle 11|), \tag{167f}$$
$$\tilde{\rho}_{10}^{\hat{n}_2}=\mathrm{tr}_{3,4}[(\mathcal{P}_{10}^{\hat{\mathrm{n}}_2}\otimes\mathbb{1})\rho(\theta)]=\frac{1}{8}(|00\rangle-\mathrm{i}|11\rangle)(\langle 00|+\mathrm{i}\langle 11|), \tag{167g}$$
$$\tilde{\rho}_{11}^{\hat{n}_2}=\mathrm{tr}_{3,4}[(\mathcal{P}_{11}^{\hat{\mathrm{n}}_2}\otimes\mathbb{1})\rho(\theta)]=\frac{1}{8}(|00\rangle+\mathrm{i}|11\rangle)(\langle 00|-\mathrm{i}\langle 11|). \tag{167h}$$

If Bob's eight unnormalized conditional states can have a LHS description, they must satisfy

$$\tilde{\rho}_{00}^{\hat{n}_1}=\sum_\xi \wp(00|zz,\xi)\wp_\xi\rho_\xi, \tag{168a}$$
$$\tilde{\rho}_{01}^{\hat{n}_1}=\sum_\xi \wp(01|zz,\xi)\wp_\xi\rho_\xi, \tag{168b}$$
$$\tilde{\rho}_{10}^{\hat{n}_1}=\sum_\xi \wp(10|zz,\xi)\wp_\xi\rho_\xi, \tag{168c}$$
$$\tilde{\rho}_{11}^{\hat{n}_1}=\sum_\xi \wp(11|zz,\xi)\wp_\xi\rho_\xi, \tag{168d}$$
$$\tilde{\rho}_{00}^{\hat{n}_2}=\sum_\xi \wp(00|yx,\xi)\wp_\xi\rho_\xi, \tag{168e}$$
$$\tilde{\rho}_{01}^{\hat{n}_2}=\sum_\xi \wp(01|yx,\xi)\wp_\xi\rho_\xi, \tag{168f}$$
$$\tilde{\rho}_{10}^{\hat{n}_2}=\sum_\xi \wp(10|yx,\xi)\wp_\xi\rho_\xi, \tag{168g}$$
$$\tilde{\rho}_{11}^{\hat{n}_2}=\sum_\xi \wp(11|yx,\xi)\wp_\xi\rho_\xi. \tag{168h}$$

From Eq. (167), we known that $\tilde{\rho}_a^{\hat{n}}$ are all proportional to pure states, thus the ensemble is

$$\{\wp_\xi\rho_\xi\}=\{\wp_1\rho_1,\wp_2\rho_2,\wp_3\rho_3,\wp_4\rho_4,\wp_5\rho_5,\wp_6\rho_6,\wp_7\rho_7,\wp_8\rho_8\}, \tag{169}$$

where $\wp_1 > 0$. So, Eq. (168) become

$$\tilde{\rho}_{00}^{\hat{n}_1} = \sum_{i=1}^{8} \wp(00|zz,i)\wp_i\rho_i, \tag{170a}$$

$$\tilde{\rho}_{01}^{\hat{n}_1} = \sum_{i=1}^{8} \wp(01|zz,i)\wp_i\rho_i, \tag{170b}$$

$$\tilde{\rho}_{10}^{\hat{n}_1} = \sum_{i=1}^{8} \wp(10|zz,i)\wp_i\rho_i, \tag{170c}$$

$$\tilde{\rho}_{11}^{\hat{n}_1} = \sum_{i=1}^{8} \wp(11|zz,i)\wp_i\rho_i, \tag{170d}$$

$$\tilde{\rho}_{00}^{\hat{n}_2} = \sum_{i=1}^{8} \wp(00|yx,i)\wp_i\rho_i, \tag{170e}$$

$$\tilde{\rho}_{01}^{\hat{n}_2} = \sum_{i=1}^{8} \wp(01|yx,i)\wp_i\rho_i, \tag{170f}$$

$$\tilde{\rho}_{10}^{\hat{n}_2} = \sum_{i=1}^{8} \wp(10|yx,i)\wp_i\rho_i, \tag{170g}$$

$$\tilde{\rho}_{11}^{\hat{n}_2} = \sum_{i=1}^{8} \wp(11|yx,i)\wp_i\rho_i, \tag{170h}$$

As we know,

$$\wp_\xi > 0, \quad \sum_\xi \wp_\xi = 1, \tag{171a}$$

$$\sum_{a,b} \wp(ab|\hat{n},\xi) = 1. \tag{171b}$$

and

$$\sum_\xi \wp_\xi\rho_\xi = \rho_{12} = \mathrm{tr}_{3,4}[\rho(\theta)] \tag{172}$$

is the reduced density matrix for Bob. According to property that a density matrix of pure state can only be expanded by itself. Without loss of generality, we suppose the Eq. (170) as

$$\tilde{\rho}_{00}^{\hat{n}_1} = \wp_1\rho_1, \tag{173a}$$
$$\tilde{\rho}_{01}^{\hat{n}_1} = \wp_2\rho_2, \tag{173b}$$
$$\tilde{\rho}_{10}^{\hat{n}_1} = \wp_3\rho_3, \tag{173c}$$
$$\tilde{\rho}_{11}^{\hat{n}_1} = \wp_4\rho_4, \tag{173d}$$
$$\tilde{\rho}_{00}^{\hat{n}_2} = \wp_5\rho_5, \tag{173e}$$
$$\tilde{\rho}_{01}^{\hat{n}_2} = \wp_6\rho_6, \tag{173f}$$
$$\tilde{\rho}_{10}^{\hat{n}_2} = \wp_7\rho_7, \tag{173g}$$
$$\tilde{\rho}_{11}^{\hat{n}_2} = \wp_8\rho_8, \tag{173h}$$

i.e.,$\wp(00|zz,1) = \wp(01|zz,2) = \wp(10|zz,3) = \wp(11|zz,4) = \wp(00|yx,5) = \wp(01|yx,6) = \wp(10|yx,7) = \wp(11|yx,8) = 1$, the other $\wp(ab|\hat{n},j) = 0$.

It can be verified that

$$\tilde{\rho}_{00}^{\hat{n}_1} + \tilde{\rho}_{01}^{\hat{n}_1} + \tilde{\rho}_{10}^{\hat{n}_1} + \tilde{\rho}_{11}^{\hat{n}_1} = \tilde{\rho}_{00}^{\hat{n}_2} + \tilde{\rho}_{01}^{\hat{n}_2} + \tilde{\rho}_{10}^{\hat{n}_2} + \tilde{\rho}_{11}^{\hat{n}_2} = \rho_{12}, \tag{174a}$$
$$\rho_{12} = \mathrm{tr}_{3,4}[\rho(\theta)] = \tfrac{1}{2}(|00\rangle\langle 00| + |11\rangle\langle 11|). \tag{174b}$$

For the Eq. (173), by summing them up and taking trace, the left-hand side gives the quantum prediction as $\mathrm{tr}_{12}(2\rho_{12}) = 2$. According to Eq. (172), the right-hand side gives the classical prediction as $\mathrm{tr}_{12}(\rho_{12}) = 1$. This leads to the sharp contradiction "$1_{\rm C} = 2_{\rm Q}$" between the LHS models and QM.

2. ADDITIONAL EXPERIMENTAL INFORMATION

A. Details about the setup and state preparation

The phase retarders on separated photon paths are d=12.7mm true-zero-order half-wave plates and quarter-wave plates, concentrically glued on d=25.4mm glass plates and installed on motorized wave-plate rotators. All of the rotators are eccentrically aligned so only one photon path intersects the phase retarder, and the other passes through the glass substrate. In this manner, phase retarders on each path can be individually adjusted. We make use of the infrared laser and a charge-coupled device (CCD) beam profiler to precisely align the wave plates. The two paths should be separated as near as possible, in order to stabilize the interference setup. $3mm$ is almost the smallest viable separation, in order to avoid possible clip of wavefunction profile at the edge of wave plates.

On the working surface of the polarized beam splitter, we assumed the reflected wavefunction acquires a $\pi/2$ additional phase to keep its Hamiltonian same as the photon fusion gate. As was mentioned in [13], it does not precisely hold in an actual experiment. However, by finely tilting the beam displacers, this additional phase can be compensated.

The cross-shaped setup appears in the main text is capable of preparing different types of entangled state. In Table.7, we present various settings to prepare the GHZ and cluster state used in the mean text, as well as a polarization-path hyper-entangled state $|\phi^+\rangle_{pol.} \otimes |\phi^-\rangle_{path}$, which also yields powerful AvN arguments with only two observers [9].

State	#1	#2	#3	#4	#5	#6
GHZ $\lvert GHZ_4(0)\rangle$	22.5	22.5	0	0	0	90
Cluster $\lvert LC_4(0)\rangle$	22.5	22.5	22.5	22.5	67.5	22.5
$\lvert\phi^+\rangle \otimes \lvert\phi^-\rangle$	22.5	22.5	67.5	67.5	67.5	67.5

Supplementary Table 7. The required optic axis orientation of HWPs in Fig. 3 in the main text to prepare 4-qubit GHZ and cluster states, as well as polarization-path hyperentangled state.

It is also possible to consider the 2×2 polarization-path qubits as an up-to-4-dimensional qudit. Every term in the prepared qudit constantly comes with a real coefficient, for the Jones matrix of half-wave plate (HWP) is real. With the same measurement apparatus in the main setup, projective measurements onto arbitrary distinct 4-qubit bases are still attainable. To prepare qudit states with complex coefficients, one may add a set of quarter-wave plate (QWP) followed by a HWP and another QWP to individually cast unitary transformations on each path mode.

B. Proposed setup for observing $m = 5$ GHZ-type paradox

The GHZ-type paradox and its related applications in our findings have profound implications in multi-qubit scenarios. For example, all of the four locally nonequivalent 5-qubit graph states can be uniquely identified by their corresponding GHZ-type paradoxes. Consequently, the related experimental investigations appear to be of particular interest. The photonic test-bed is suitable for the generation and manipulation of graph state [10, 11], and here we provide the recipe for the generation of all these states.

According to the definition of the graph state, the explicit form of a m-qubit graph state $|G\rangle$ can be expressed as

$$|G\rangle = \left(\bigotimes_{C_i^j=1} CZ_i^j \right) |+\rangle^{\otimes m},$$

where CZ_i^j is the controlled-z interaction between the qubits i and j, and $|+\rangle = (|0\rangle + |1\rangle)/\sqrt{2}$ is the single-qubit maximal superposition state. In other words, all graph states can in principle be prepared by initializing all qubits on the maximal superposition state, and applying controlled-z gate between the qubits corresponding to the connected vertices. However, the controlled-z operation in linear optics system requires postselection by coincidence counting [12], and it cannot be repeatedly applied on multiple qubits to form a "closed loop", and thus is not solely competent to generate the graph states whose graph representation is cyclic. The same obstacle also exists in the case of the PBS gate. Nevertheless, this can be remedied using the additional entanglement generated by spontaneous parametric down-conversion. As the efficiency of the controlled-Z gate on two maximal superposition states is 1/9 and the PBS gate is 1/2, the latter is more preferred for generation of bright multi-qubit graph states.

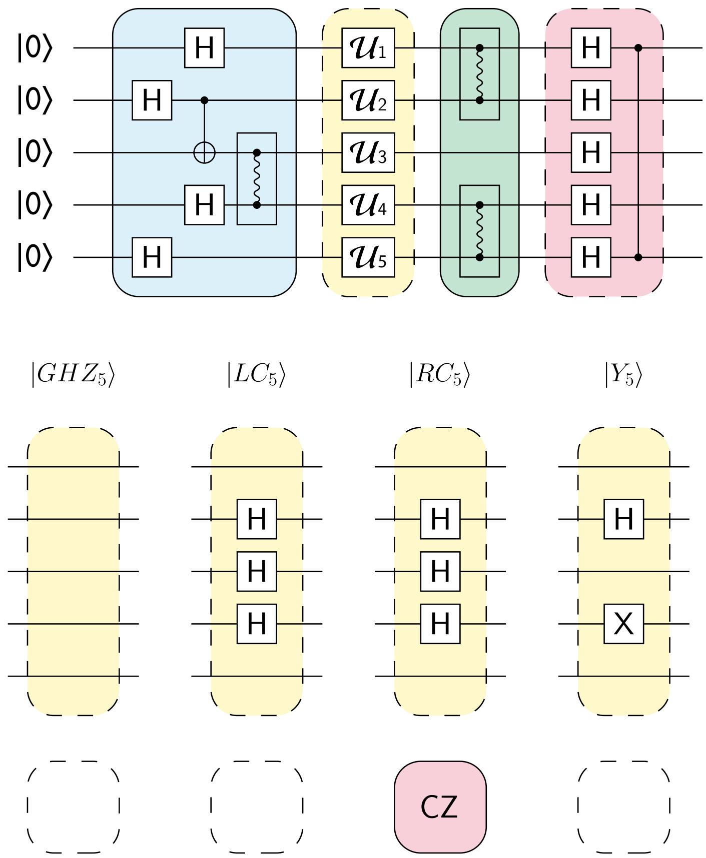

Supplementary Figure 5. A unified quantum circuits for generation of 5-qubits graph states. The tilde line inside a box that connect two qubits denote the PBS gate, and the other logical gates use standard quantum circuit notations. $\mathcal{U}_1 \sim \mathcal{U}_5$ are local operations that can be Hadamard (H), NOT (X) and identity (not shown), as is displayed in the yellow colored subplot. Only generation of the ring cluster state $|RC_5\rangle$ requires the final controlled-Z gate.

Fig. 5 shows a possible quantum circuit which requires only one pair of Bell states and at most one controlled-Z gate to generate all 5-qubit graph states, and its photonic implementation can be found in Fig. 6. The correspondences of the same parts of quantum circuits are denoted by the colors. In this setup, the qubits are all encoded in the polarization degree of freedom of the photons. The parametric photon source in the middle of the blue rounded rectangle generates maximally entangled photons, and the top and bottom ones only prepares time-correlated single photon pairs, initialized in maximal superposition state, with one of the photons from the top parametric source are taken as a herald. The photons #3 and #4 are then immediately affected by a PBS gate.

In the yellow rounded rectangle, the three HWPs implement the local unitaries, and the orientation of the wave plates for the photons {#2, #3 and #4} should be set to $\{0°, 0°, 0°\}$, $\{22.5°, 22.5°, 22.5°\}$, $\{22.5°, 22.5°, 22.5°\}$, and $\{45°, 0°, 22.5°\}$ in order to prepare the GHZ state $|GHZ_5\rangle$, linear cluster state $|LC_5\rangle$, ring cluster state $|RC_5\rangle$, and the Y-state $|Y_5\rangle$, respectively. At this point, interfering the photon pairs {#1, #2} and {#4, #5} again on two PBS gates suffices to prepare the $|GHZ_5\rangle$, $|LC_5\rangle$ and $|Y_5\rangle$ states (up to some local unitary operations). Furthermore, the qubits #1 and #5 can still be affected by the controlled-Z gate, so applying the gate on $|LC_5\rangle$ finally generates the ring cluster state $|RC_5\rangle$. Additionally, the controlled-Z gate can be constructed using three partially polarizing beam splitters (PPBSs), which have reflectivities of 1/3 and 1 for horizontally and vertically polarized photons, respectively, and some additional HWPs [12]. This gate is displayed in the block with magenta background.

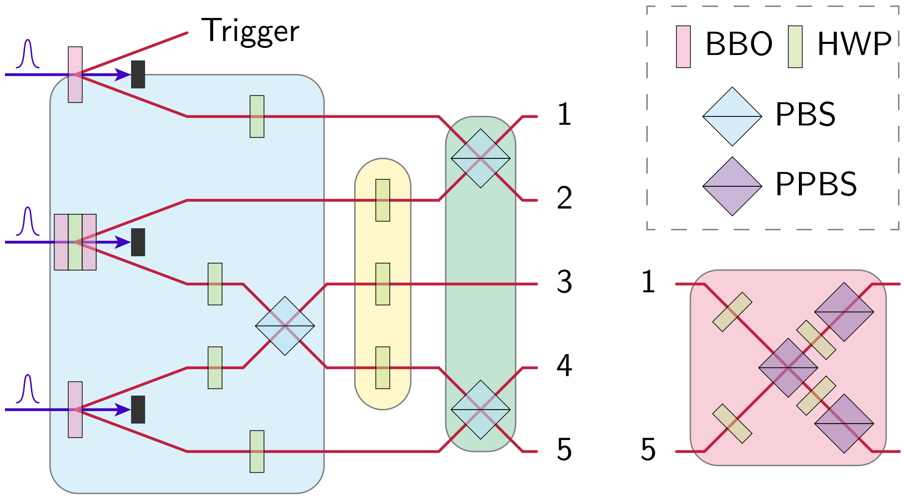

Supplementary Figure 6. Photonic realization of the quantum circuit in Fig. 5 for the generation of all 5-qubit graph states.

Wave plates configuration	CZ gate	Final state $\lvert 0\rangle \leftrightarrow \lvert H\rangle, \lvert 1\rangle \leftrightarrow \lvert V\rangle$	Equivalent graph state	Operators in GHZ-type paradox
$\{0^\circ, 0^\circ, 0^\circ\}$	no	$\frac{1}{\sqrt{2}}(\lvert 00000\rangle + \lvert 11111\rangle)$	$= \lvert G_5\rangle$	$\{\sigma_y\sigma_y\sigma_x\sigma_x\sigma_x,\ \sigma_x\sigma_y\sigma_y\sigma_x\sigma_x,\ \sigma_x\sigma_x\sigma_y\sigma_y\sigma_x,\ \sigma_x\sigma_x\sigma_x\sigma_y\sigma_y,\ \sigma_y\sigma_x\sigma_x\sigma_x\sigma_y,\ \sigma_x\sigma_x\sigma_x\sigma_x\sigma_x\}$
$\{22.5^\circ, 22.5^\circ, 22.5^\circ\}$	no	$\frac{1}{2}(\lvert 00011\rangle - \lvert 00100\rangle + \lvert 11000\rangle - \lvert 11111\rangle)$	$= (\sigma_x H \otimes H \otimes H\sigma_x \otimes \mathbb{1} \otimes H) \lvert LC_5\rangle$	$\{\sigma_x\sigma_y\sigma_z\sigma_y\sigma_x,\ \mathbb{1}\sigma_z\sigma_y\sigma_y\sigma_x,\ \sigma_x\sigma_y\sigma_y\sigma_z\mathbb{1},\ \sigma_z\sigma_z\mathbb{1}\mathbb{1}\mathbb{1},\ \sigma_z\mathbb{1}\sigma_z\mathbb{1}\sigma_z,\ \mathbb{1}\mathbb{1}\mathbb{1}\sigma_z\sigma_z\}$
$\{22.5^\circ, 22.5^\circ, 22.5^\circ\}$	yes	$\frac{1}{2\sqrt{2}}(\lvert 00100\rangle + \lvert 00111\rangle - \lvert 01001\rangle - \lvert 01010\rangle + \lvert 10001\rangle - \lvert 10010\rangle + \lvert 11100\rangle - \lvert 11111\rangle)$	$= (\sigma_y \otimes H\sigma_y \otimes \sigma_x \otimes H \otimes \sigma_z) \lvert RC_5\rangle$	$\{\sigma_z\sigma_y\sigma_x\sigma_y\sigma_z,\ \sigma_z\sigma_z\sigma_z\mathbb{1}\mathbb{1},\ \mathbb{1}\mathbb{1}\sigma_z\sigma_z\sigma_z,\ \sigma_y\sigma_z\sigma_x\sigma_y\mathbb{1},\ \sigma_y\mathbb{1}\sigma_x\mathbb{1}\sigma_y,\ \mathbb{1}\sigma_y\sigma_x\sigma_z\sigma_y\}$
$\{22.5^\circ, 0^\circ, 45^\circ\}$	no	$\frac{1}{2}(\lvert 00011\rangle - \lvert 00100\rangle - \lvert 11011\rangle - \lvert 11100\rangle)$	$= (H \otimes \mathbb{1} \otimes \sigma_x \otimes H \otimes H\sigma_x) \lvert Y_5\rangle$	$\{\sigma_x\sigma_y\sigma_y\sigma_x\sigma_x,\ \sigma_y\sigma_y\sigma_z\mathbb{1}\mathbb{1},\ \mathbb{1}\mathbb{1}\sigma_z\mathbb{1}\sigma_z,\ \sigma_y\sigma_x\sigma_y\sigma_x\sigma_x,\ \sigma_x\sigma_x\mathbb{1}\sigma_z\mathbb{1},\ \mathbb{1}\mathbb{1}\mathbb{1}\sigma_z\sigma_z\}$

Supplementary Table 8. Summary of the preparation of 5-qubit graph states and their corresponding GHZ-type paradoxes.

C. Effect of sequential measurements

The behavior of out tested models should be given by quantum correlations. While demonstrating the sharp contradiction between QM and LHV models, to ascribe the observed phenomena solely to QM, one is obliged to test nonsignaling condition of sequential measurements, which rules out superquantum correlations induced by signaling between ideally spacelike measurements. Formally, the nonsignaling condition requires

$$\forall\ x, y, z, ..., y', z', ..., \qquad \sum_{i,j,...} P(a, b_i, c_j, ...|x, y, z, ...) = \sum_{i,j,...} P(a, b'_i, c'_j|x, y', z', ...). \tag{175}$$

Where $a, b_i, c_j, ..., b'_i, c'_j, ...$ denote measurement results, and $x, y, z, ..., y', z', ...$ stand for measurement settings.

In this experiment, because the observable set contains both path and polarization variables, the requirements of non-signaling condition are two-folded, that 1) the local marginal probabilities of Alice should be independent of Bob's measurement settings, and vice versa, and that 2) the marginal probabilities of Alice's sequential measurements should be independent of each other, regardless of the other measurement is done prior or posterior in time. The form of the sharp contradictions guarantees that any individual observables in this scheme, e.g., σ_x^1, appears at least two times. This allows us to compare the two marginal probabilities under two complete measurements, and check their consistency.

We compare the same observable's expectation values deduced from different sets of complete measurement. Principally, these results may be affected by the other photon's measurement choices, as well as the measurements im-

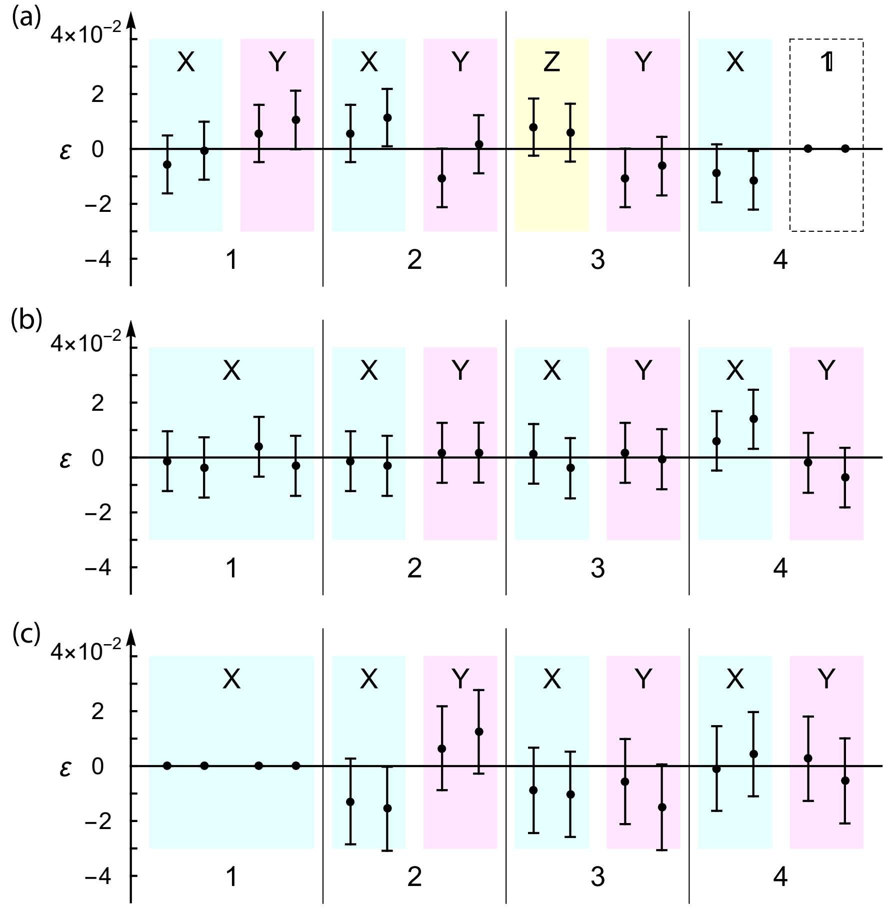

Supplementary Figure 7. Marginal probabilities deviation of various observables from theoretical value, serving to check the nonsignaling condition. Plots (a) (b) and (c) are calculated from measurement results for states $|LC_4(0)\rangle$, $|GHZ_4(0)\rangle$, and $|GHZ_4(\pi/4)\rangle$, respectively. The measurement results provide at least two ways to determine the marginal probabilities for each individual observable, which is denoted by degree of freedom indices (1-4) and measurement choices (X stands for σ_x, Y for σ_y, Z for σ_z and $\mathbb{1}$ for identity). The error bars are calculated by Poisson counting statistics and stand for 1σ stanndard deviation. The $|GHZ_4(\pi/4)\rangle$ state is prepared by postselecting $\langle\sigma_x\rangle = 1$ ensembles, which gives rise to the zero value and null error bar of corresponding data points.

plemented on the same photon's other degrees of freedom. The results are shown in Fig. 7. Calculated marginal probability deviations from theoretical value indicate that the expectation values of observables are approximately identical for different joint measurement settings. The expectation values determined for the same observable always fall in each others' error bars, which well agrees with the requirements of nonsignaling constraint.

D. Experimental determination of steering parameter $\mathcal{I}_s$

In this work, quantum steering is observed by a significant violation of $\mathcal{I}_s = 1$ to reject the hybrid LHV/LHS model, and $\mathcal{I}_s = \mathrm{Tr}\sum_{\mu,\nu}\tilde{\rho}_{\mu}^{\nu}$. By exploiting the perfect correlation between the conditional states and the Pauli observables, a lower bound of $\mathcal{I}_s$ can be experimentally determined. Without loss of generality, here we explain the procedure of extracting a lower bound of $\mathrm{Tr}\tilde{\rho}_{00}^{\hat{n}_1}$ in (168a).

Because the theoretical conditional state is an eigenstate of $\sigma_x\sigma_x - \sigma_y\sigma_y$ with an eigenvalue of 2, meanwhile, the other eigenvalues of $\sigma_x\sigma_x - \sigma_y\sigma_y$ are non-positive. This is very similar to the situation in the above application of "entanglement detection". As such, we expand the conditional density matrix with at most four pure states, namely, $\mathrm{Tr}\tilde{\rho}_{00}^{\hat{n}_1} = \sum_{i=1}^{4}\lambda_i\,|\tilde{\psi}_i\rangle\,\langle\tilde{\psi}_i|$. Furthermore, the eigenstates of $\sigma_x\sigma_x - \sigma_y\sigma_y$ are denoted by $|\psi_1\rangle\,, |\psi_2\rangle\,, |\psi_3\rangle\,, |\psi_4\rangle$ with their eigenvalues being {2, 0, 0, -2}, respectively. Then,

$$\begin{aligned}
\mathrm{Tr}\left[\tilde{\rho}_{00}^{\hat{n}_1}(\sigma_x\sigma_x-\sigma_y\sigma_y)\right] &= \mathrm{Tr}\left[\sum_{i=1}^{4}\lambda_i\,|\tilde{\psi}_i\rangle\,\langle\tilde{\psi}_i|\,(\sigma_x\sigma_x-\sigma_y\sigma_y)\right] \\
&= \mathrm{Tr}\left[\sum_{i,j,k=1}^{4}\lambda_i c_{ij}c_{ik}^{*}\,|\psi_j\rangle\,\langle\psi_k|\,(\sigma_x\sigma_x-\sigma_y\sigma_y)\right] \\
&= \mathrm{Tr}\left[\sum_{i,j=1}^{4}\lambda_i|c_{ij}|^2\,|\psi_j\rangle\,\langle\psi_j|\,(\sigma_x\sigma_x-\sigma_y\sigma_y)\right] \\
&\leq \mathrm{Tr}\left[\sum_{i=1}^{4}\lambda_i|c_{i1}|^2\,|\psi_1\rangle\,\langle\psi_1|\,(\sigma_x\sigma_x-\sigma_y\sigma_y)\right] \\
&\leq 2\sum_{i=1}^{4}\lambda_i. \qquad (176)
\end{aligned}$$

The two inequalities hold because (1) the other eigenvalues of $(\sigma_x\sigma_x-\sigma_y\sigma_y)$ are non-positive, and (2) the modular square of the four coefficients $\sum_j|c_{ij}|^2=1$. The quantity $\mathrm{Tr}\left[\tilde{\rho}_{00}^{\hat{n}_1}(\sigma_x\sigma_x-\sigma_y\sigma_y)\right]$, on the other hand, is experimentally calculated using the recorded event counts. For example, in (168a), let N_{xyzw}^{abcd} denote the recorded event counts of obtaining outcomes a,b,c,d when the measurement settings for the four qubits are x,y,z,w, respectively, and $N_{\_\_zw}^{\_\_cd}$ denote the recorded event counts of obtaining outcomes c,d when the measurement settings for the last two qubits are z,w and the first two qubits are not measured. Then,

$$\begin{aligned}
\mathrm{Tr}\left[\tilde{\rho}_{00}^{\hat{n}_1}(\sigma_x\sigma_x-\sigma_y\sigma_y)\right] = {}&\left(\frac{N_{xxzz}^{++++}+N_{xxzz}^{--++}-N_{xxzz}^{+-++}-N_{xxzz}^{-+++}}{N_{xxzz}^{++++}+N_{xxzz}^{--++}+N_{xxzz}^{+-++}+N_{xxzz}^{-+++}}-\frac{N_{yyzz}^{++++}+N_{yyzz}^{--++}-N_{yyzz}^{+-++}-N_{yyzz}^{-+++}}{N_{yyzz}^{++++}+N_{yyzz}^{--++}+N_{yyzz}^{+-++}+N_{yyzz}^{-+++}}\right) \\
&\times\frac{N_{__zz}^{__++}}{N_{__zz}^{__++}+N_{__zz}^{__+-}+N_{__zz}^{__-+}+N_{__zz}^{__--}}, \qquad (177)
\end{aligned}$$

and the other traces of conditional density matrices $\tilde{\rho}_{ij}^{\hat{n}}$'s are extracted very similarly.

---

[1] L. Hardy, Nonlocality for two particles without inequalities for almost all entangled states. Phys. Rev. Lett. **71**, 1665 (1993).

[2] J. L. Chen, A. Cabello, Z. P. Xu, H. Y. Su, C. Wu, and L. C. Kwek, Hardy's paradox for high-dimensional systems, Phys. Rev. A **88**, 062116 (2013).

[3] M. Yang, H.-X. Meng, J. Zhou, Z.-P. Xu, Y. Xiao, K. Sun, J.-L. Chen, J.-S. Xu, C.-F. Li, and G.-C. Guo, Stronger Hardy-type paradox based on the Bell inequality and its experimental test Phys. Rev. A **99**, 032103 (2019).

[4] D. M. Greenberger, M. A. Horne and A. Zeilinger, arXiv preprint 0712.0921, in *Bell's Theorem, Quantum Theory, and Conceptions of the Universe*, M. Kafatos (Ed.), Kluwer, Dordrecht, 69-72 (1989).

[5] H. M. Wiseman, S. J. Jones, and A. C. Doherty, Steering, Entanglement, Nonlocality, and the Einstein-Podolsky-Rosen Paradox, Phys. Rev. Lett. **98**, 140402 (2007).

[6] J. L. Chen, H. Y. Su, Z. P. Xu, and A. K. Pati, Sharp Contradiction for Local-Hidden-State Model in Quantum Steering, Sci. Rep. **6**, 32075 (2016).

[7] J. C. Adcock, S. Morley-Short, A. Dahlberg, and J. W. Silverstone, arXiv preprint 1910.03969 (2019).

[8] M. Hein, J. Eisert, and H. J. Briegel, Phys. Rev. A **69**, 062311 (2004).

[9] A. Cabello, Phys. Rev. Lett. **95** 210401 (2005).

[10] D. E. Browne and T. Rudolph, Phys. Rev. Lett. **95**, 010501 (2005).

[11] T. P. Bodiya and L.-M. Duan, Phys. Rev. Lett. **97**, 143601 (2006).

[12] N. K. Langford, T. J. Weinhold, R. Prevedel, K. J. Resch, A. Gilchrist, J. L. O'Brien, G. J. Pryde, and A. G. White, Phys. Rev. Lett. **95**, 210504 (2005).

[13] Z.-Y. J. Ou, *Multi-Photon Quantum Interference* (Vol. 43), Springer, 2007.